

# A study and development of real-time strontium-90 counters based on Cherenkov radiation detection

チェレンコフ検出に基づいたリアルタイムストロンチウム90カウンターの開発研究

Hiroshi Ito  
Graduate School of Science, Chiba University

伊藤博士  
千葉大学理学研究科基盤理学専攻 物理学コース 博士後期課程3年次

# Contents

1. Introduction
2. Basic concept of an aerogel Cherenkov detector using wavelength-shifting fibers
3. Background study of environmental radiation
4. Design of a prototype detector
5. Performance of the prototype detector
6. Summary

# 1. Introduction

# 1. Introduction

- Fukushima Nuclear Accident, March, in 2011.
- $^{90}\text{Sr}$  ( $\tau_{1/2}=28.8$  yr) and  $^{137}\text{Cs}$  ( $\tau_{1/2}=30.2$  yr) are focused in the recent study.
- Decay chain:  $^{90}\text{Sr} \rightarrow ^{90}\text{Y} \rightarrow ^{90}\text{Zr}$ .
- $^{90}\text{Y}$  radioactivity is close to that of  $^{90}\text{Sr}$  by radioactive equilibrium.
- Strontium is an alkali earth metal and tends to accumulated into the bone.
- Measurement of 10-Bq/kg  $^{90}\text{Sr}$  is required rapidly.

Dose coefficient by ICRP publ.

	$^{90}\text{Sr}$ ( $^{90}\text{Y}$ )	$^{137}\text{Cs}$
Eff. Coeff. (Sv/Bq) (Adult)	$2.4 \times 10^{-8}$	$4.6 \times 10^{-9}$
Red Marrow		
Dose Coeff. (Sv/Bq) (Adult)	$1.6 \times 10^{-7}$	$4.4 \times 10^{-9}$
(Infant)	$8.6 \times 10^{-7}$	$6.8 \times 10^{-9}$

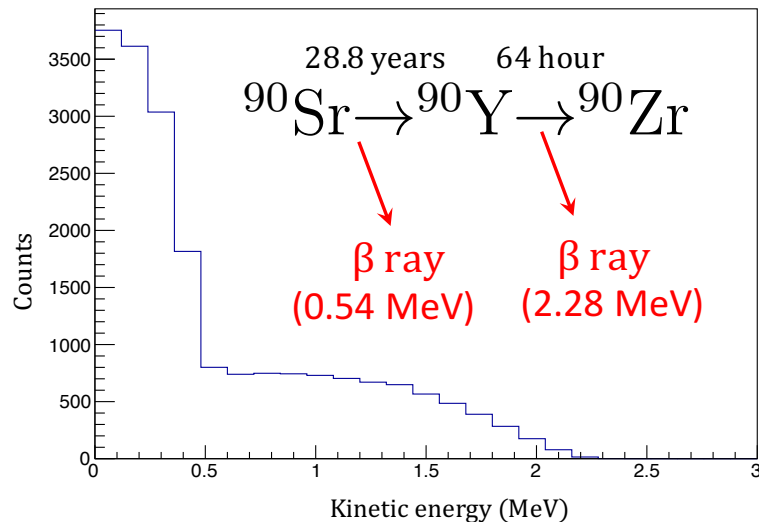


Fig. 1.1: Energy spectrum of  $\beta$  ray from  $^{90}\text{Sr}$  and  $^{90}\text{Y}$ .

# 1. Introduction

## 1.1. Conventional method of $^{90}\text{Sr}$ radioactivity measurement

- Conventional method based on a Chemical extraction.
  - Sample is burned and become ash, it takes to measure a few week – a month.
  - It is difficult to measure  $^{90}\text{Sr}$  concentration of raw-fresh foods rapidly.
- End-point method
  - Magnetic Spectrometer, Calorimeter.
  - It is difficult to determine the end-point because Environmental radiation make be background noise.
- Range method
  - Counting  $\beta$  and  $\gamma$  rays, non-calorimeter, suppressing  $\beta$  rays with low energy.
  - Lower limit: a few Bq/g in 10-min measuring (500-1000 Bq/kg @1-h measuring).
- Cherenkov radiation method
  - Using silica aerogel ( $n=1.047$ ),  $\text{Eff.}(\beta(^{137}\text{Cs}))/\text{Eff.}(\beta(^{90}\text{Y})) = (2-4) \times 10^{-2}$  .
  - An effective area:  $5 \times 5 \text{ cm}^2$ , detection limit of 0.3 Bq.
  - $^{40}\text{K}$  is most background

# 1. Introduction

## 1.2. This study and motivations

Purpose: measurement of 10 Bq/kg  $^{90}\text{Sr}$  at 1 hour in environmental radiation such as  $^{40}\text{K}$ .

Precise  $\beta$  rays inspection = Large size detection

e.g.  $100 \times 20 \text{ cm}^2$

Sample 1 kg (5-mm thick)

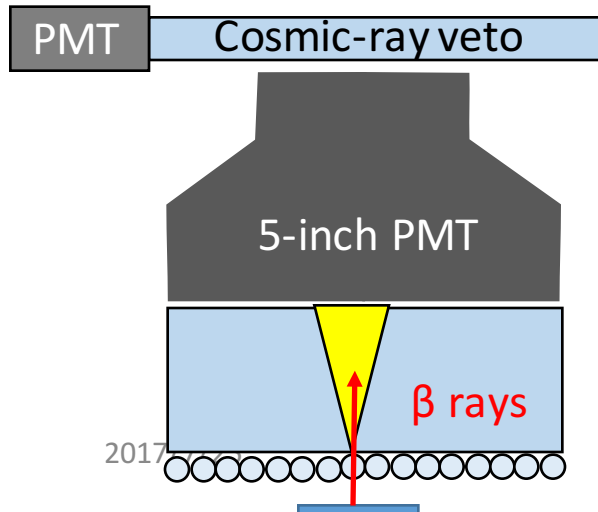
10 Bq/kg

0.1% eff.



BG rate should be less than a few count rate at 1 hour for detection 10-Bq  $^{90}\text{Sr}$  significantly.

First Type 1. Direct PMT



Count rate is more than 100 cph.

- PMT thermal noise is a few kHz.
- Accidental  $\gamma$  noises

It is not possible to inspect  $^{90}\text{Sr}$  precisely by using a large PMT.

- 1) Ring Image Cherenkov (RICH)  
... cost, Cherenkov angle =  $11.4^\circ$ , noise rate.
- 2) Reduce the amount of substance of photo-device.  
... using wavelength-shifting fibers, threshold type.

# 1. Introduction

## 1.2. This study and motivations

- I developed a threshold-type Cherenkov detector to measure  $^{90}\text{Sr}$  concentration using silica aerogel ( $n=1.041$ ) and wavelength-shifting fibers.
- I studied a basic mechanism of the Cherenkov detector.
- I studied background of environmental radiation, particularly  $^{214}\text{Bi}$  as the radon progenies.
- I produced a prototype detector with  $S=300\text{ cm}^2$ .
- The performance was estimated using radioactive sources.

## 2. Basic concept an aerogel Cherenkov detector using wavelength-shifting fibers



## 2. Basic concept an aerogel Cherenkov detector using wavelength-shifting fibers

### Cherenkov radiation

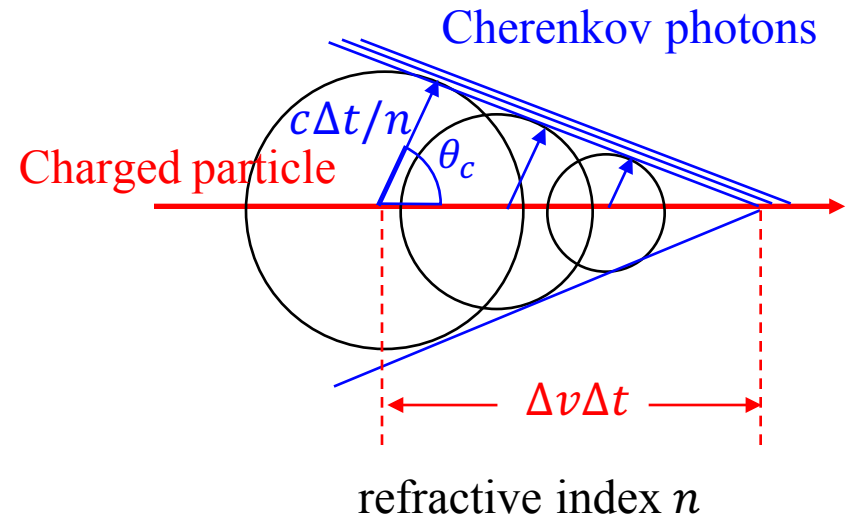
It is required for  $^{40}\text{K}$   $\beta$  rays to not emit Cherenkov photons.

A threshold of refractive index is given as

$$n_{\text{th}} = \frac{c}{v} = \frac{E}{pc} = \frac{m_e c^2 + K}{\sqrt{(m_e c^2 + K)^2 - m_e^2 c^4}}$$

where  $m_e$  is electron mass,  $K$  is  $\beta$  ray kinetic energy (MeV). In a case of  $K = 1.31$  MeV,  $n_{\text{th}} = 1.041$ .

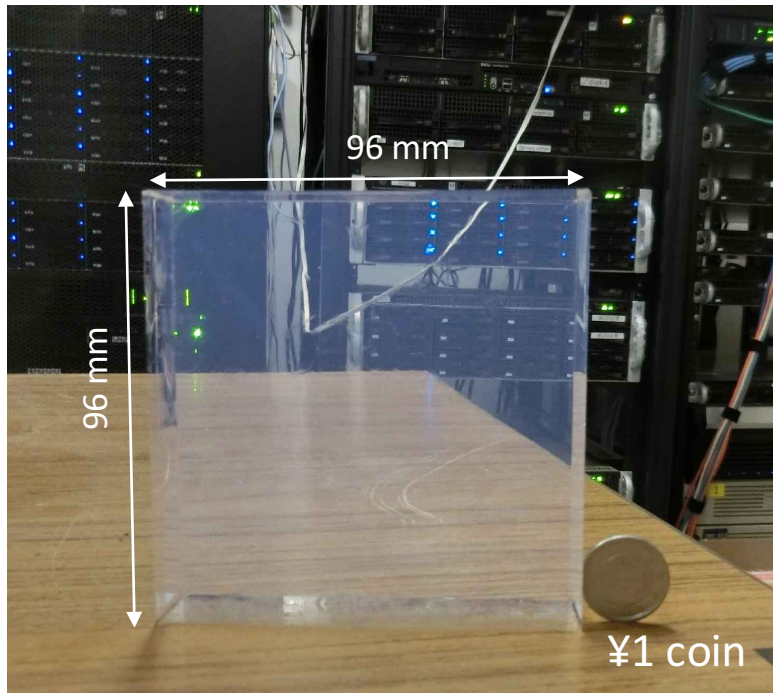
In this index, knocked out  $e^-$  by Compton scattering of  $\gamma$  ray with  $E_\gamma < 1.53$  MeV is not satisfy the Cherenkov condition in the areogel.



$$\cos\theta_c = \frac{c}{nv} < 1$$

## 2. Basic concept an aerogel Cherenkov detector using wavelength-shifting fibers

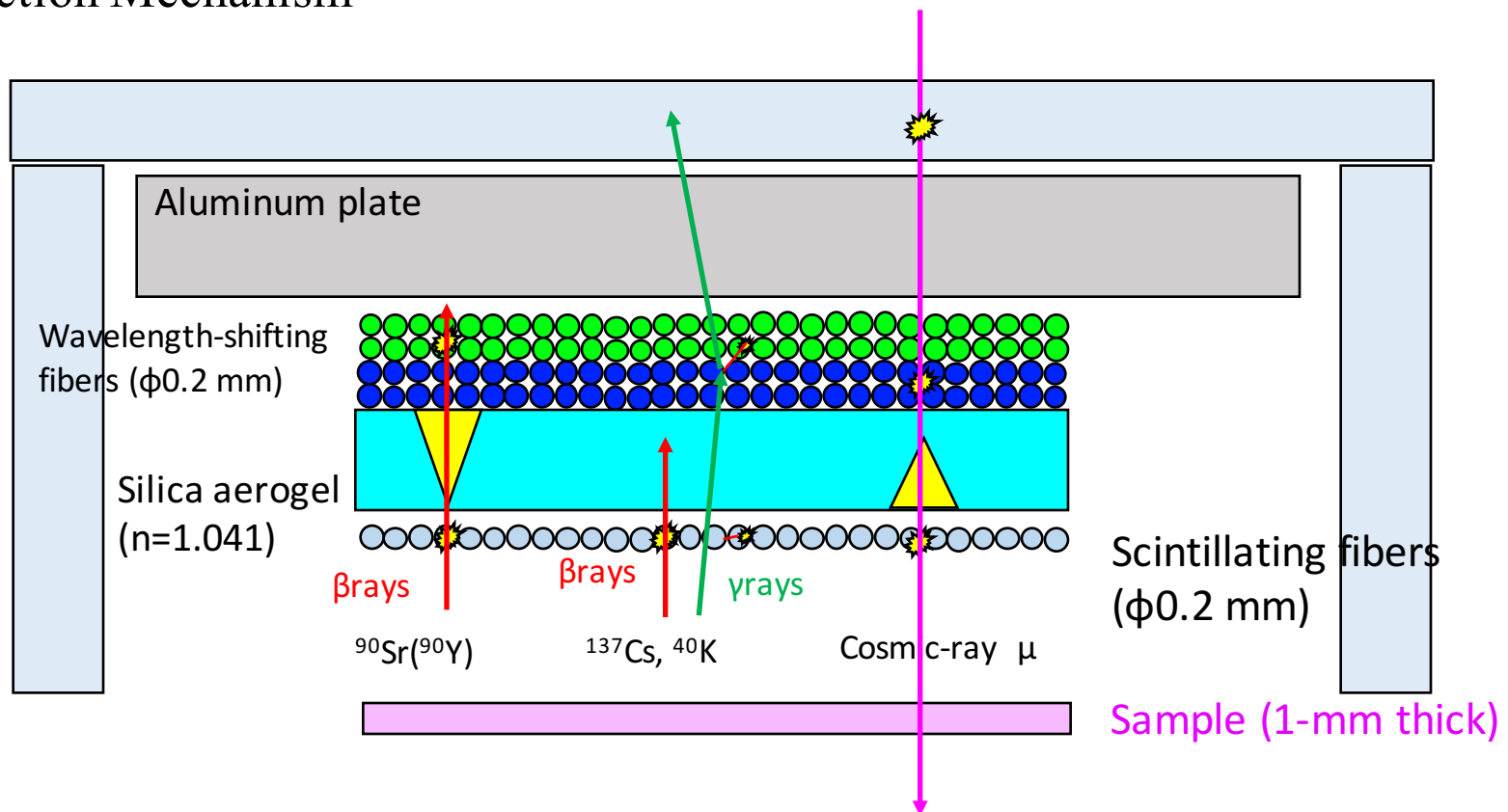
### Silica aerogel



- Silica aerogel is a material as  $\text{SiO}_2 + \text{Air}$ .
- Properties:
  - (1) Low density ( $0.1 \sim 0.2 \text{ g/cm}^3$ )
  - (2) Low refractive index
  - (3) high transparency for the visible light
- Index control:  $1.003 < n < 1.25$
- Without a hydrophilic properties by a hydrophobic treatment

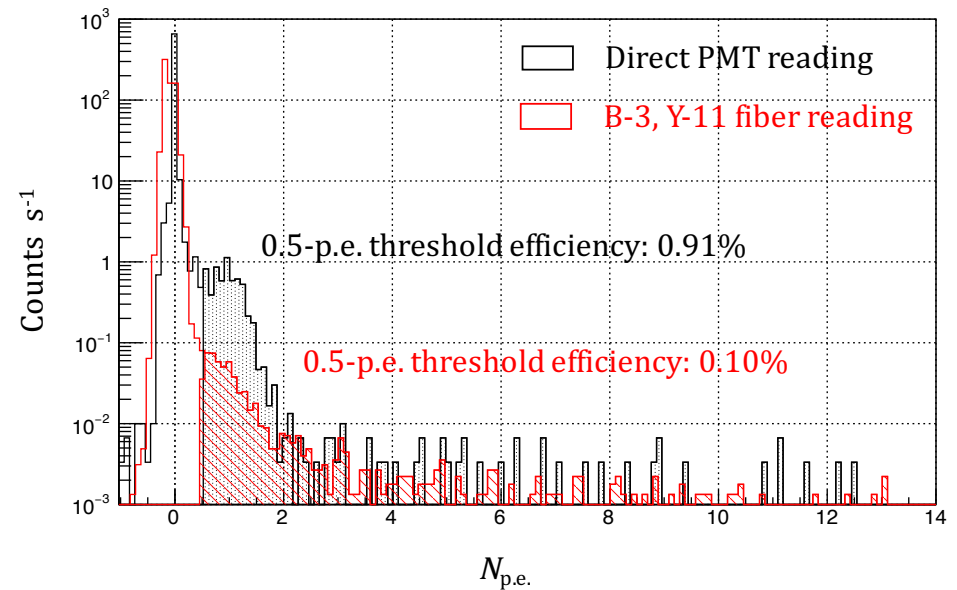
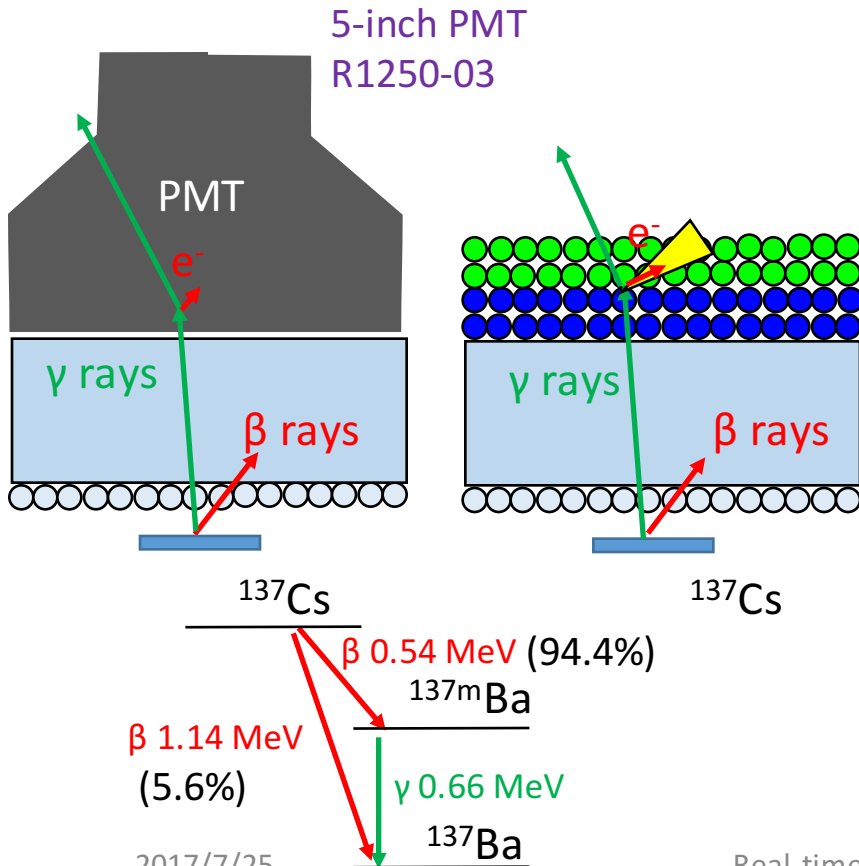
## 2. Basic concept an aerogel Cherenkov detector using wavelength-shifting fibers

### Detection Mechanism



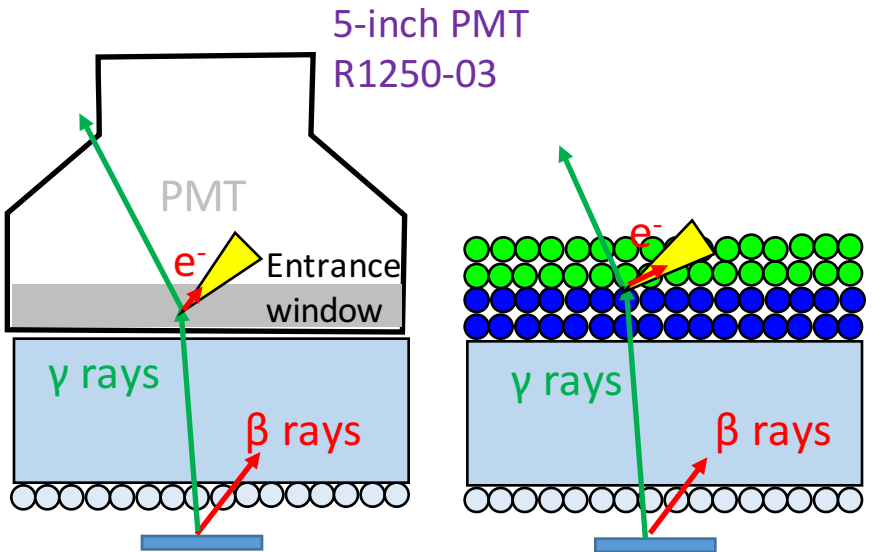
## 2. Basic concept an aerogel Cherenkov detector using wavelength-shifting fibers

Accidental noise by  $^{137}\text{Cs}$   $\gamma$  rays

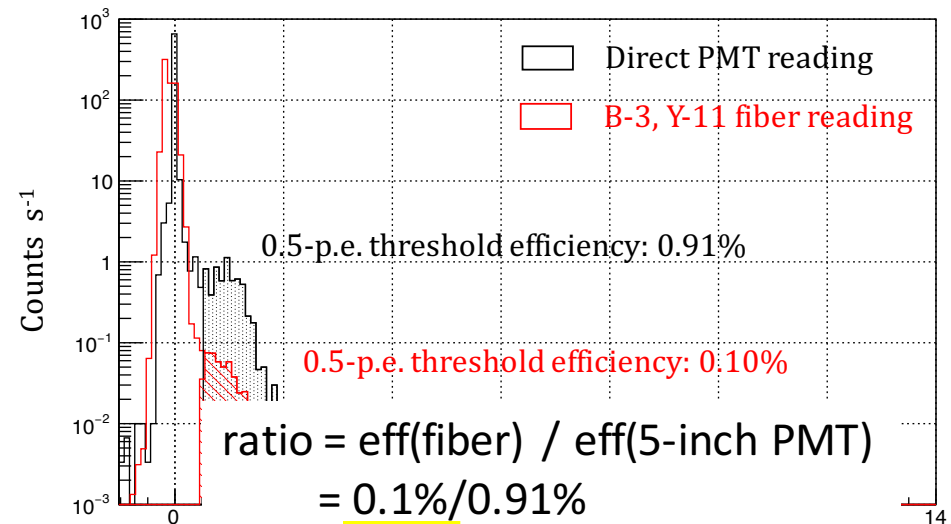


## 2. Basic concept an aerogel Cherenkov detector using wavelength-shifting fibers

Accidental noise by  $^{137}\text{Cs}$   $\gamma$  rays



	Thickness	Density
5-inch PMT entrance window	2-3 mm	2.6 g/cm <sup>3</sup>
B-3 & Y-11 sheets	0.8 mm	1.06 g/cm <sup>3</sup>



$$\begin{aligned} \text{ratio} &= \text{eff}(\text{fiber}) / \text{eff}(5\text{-inch PMT}) \\ &= 0.1\% / 0.91\% \\ &= 0.11 \end{aligned}$$



$$\begin{aligned} \text{ratio} &= \frac{0.8 \text{ mm}}{1.06 \text{ g/cm}^3} \div \frac{2\text{-}3 \text{ mm}}{2.6 \text{ g/cm}^3} \\ &= 0.11\text{-}0.16 \end{aligned}$$

## 2. Basic concept an aerogel Cherenkov detector using wavelength-shifting fibers

Optical models

Cherenkov photons

- Optical models were developed to understand wavelength-shifting fibers collection system for Cherenkov photons by reading PMT.
- The model's parameters fixed with experimental data.
- Collection efficiency of the fibers was estimated using the models.

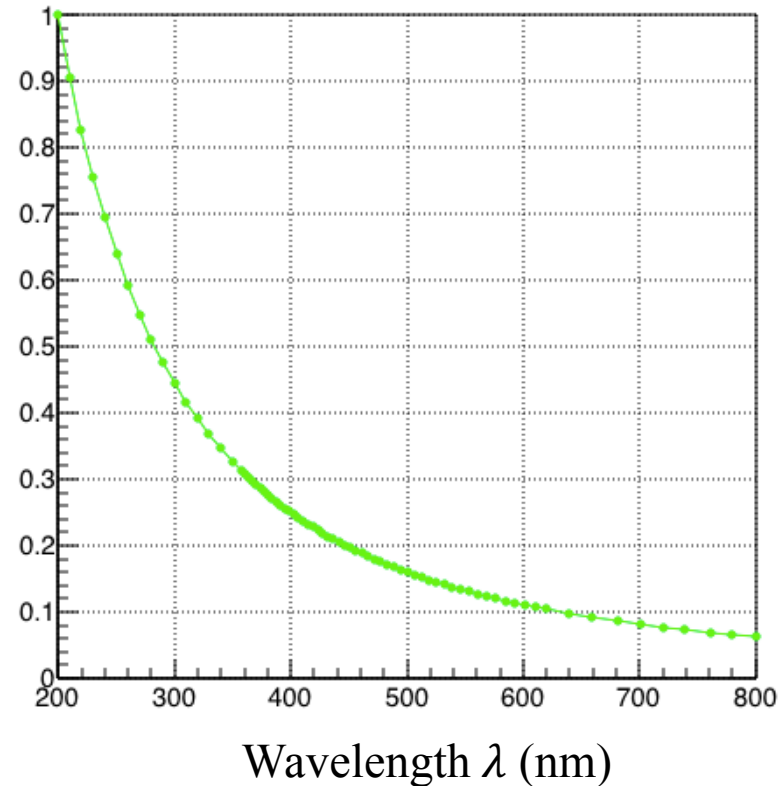
## 2. Basic concept an aerogel Cherenkov detector using wavelength-shifting fibers

Optical models  
Cherenkov photons

The number of emitted photons is given as

$$N = 2\pi\alpha L \left(1 - \frac{1}{n^2\beta^2}\right) \int_{200}^{800} \frac{d\lambda}{\lambda^2}$$

where  $\alpha$  is fine-structure constant,  $L$  is path length of the particle,  $\beta = v/c$ ,  $\lambda$  is the wavelength of emitted photons.



## 2. Basic concept an aerogel Cherenkov detector using wavelength-shifting fibers

Optical models

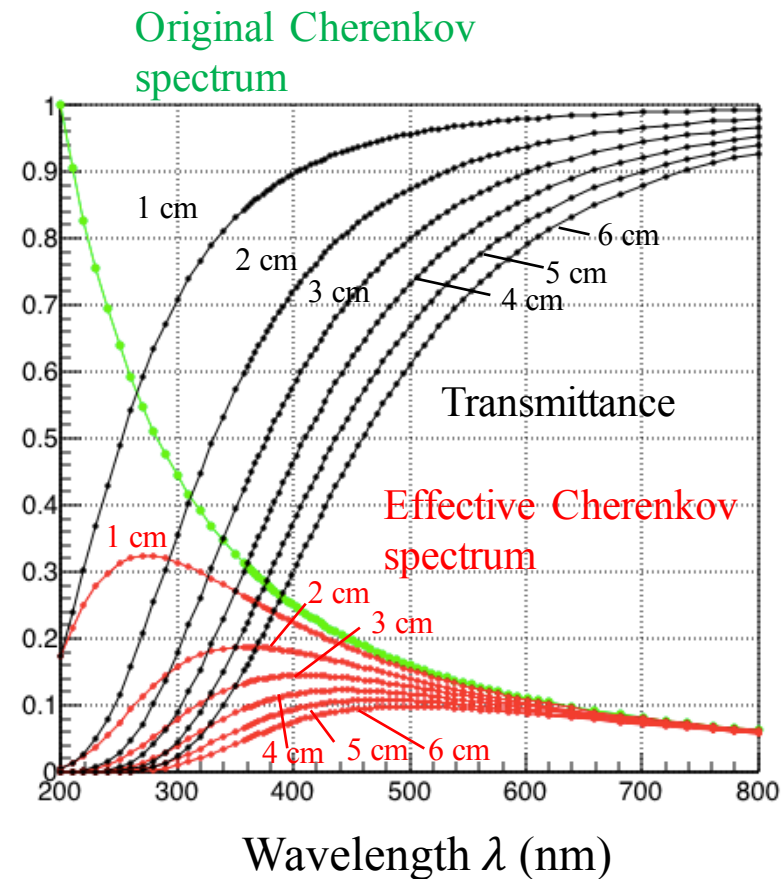
Silica aerogel transmittance

- The transmittance  $T(\lambda)$  is given as

$$T(\lambda) = A \exp\left(\frac{-Ct}{\lambda^4}\right),$$

where the amplitude is  $A=1$ ,  $C = 5.33 \pm 0.03 \mu\text{m}/\text{cm}$ ,  $t = 1\text{--}6 \text{ cm}$ .

- The effective Cherenkov spectrum has a peak at 300–500 nm



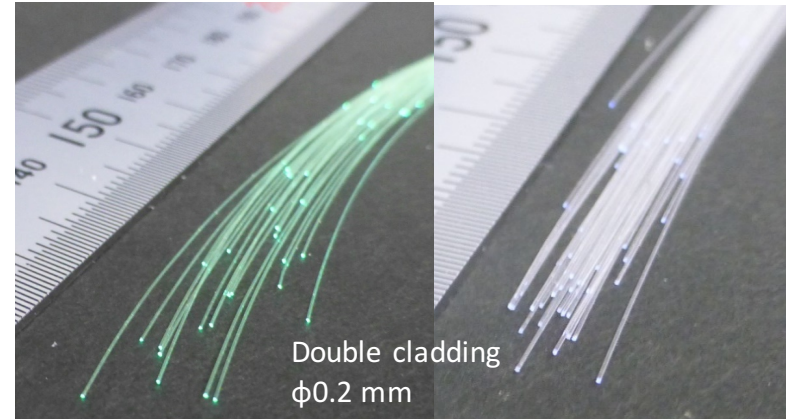


## 2. Basic concept an aerogel Cherenkov detector using wavelength-shifting fibers

### Optical models

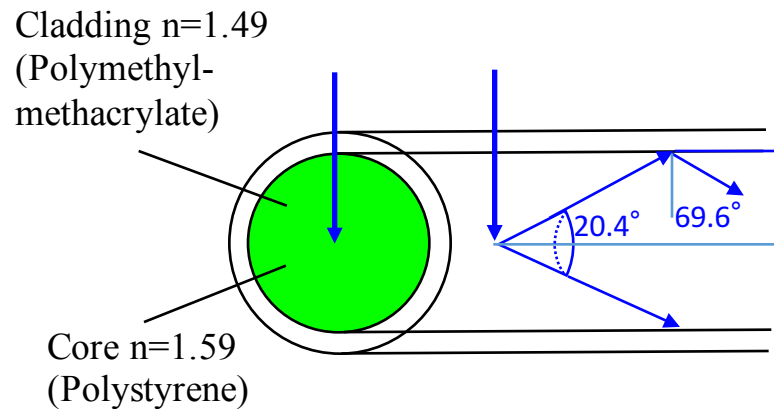
#### Wavelength-shifting fibers

- Optical plastic fibers
- Trapping efficiency determined by a ratio between a refractive indices of core and cladding.

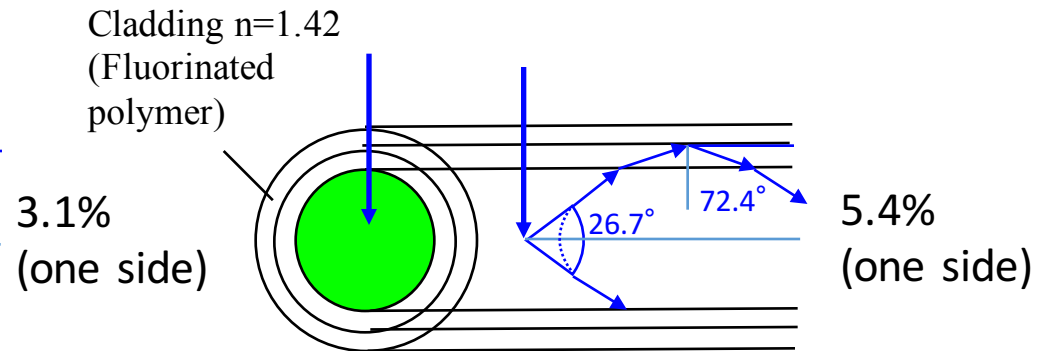


Kuraray Y-11(300)MJ

B-3(300)MJ



Single cladding

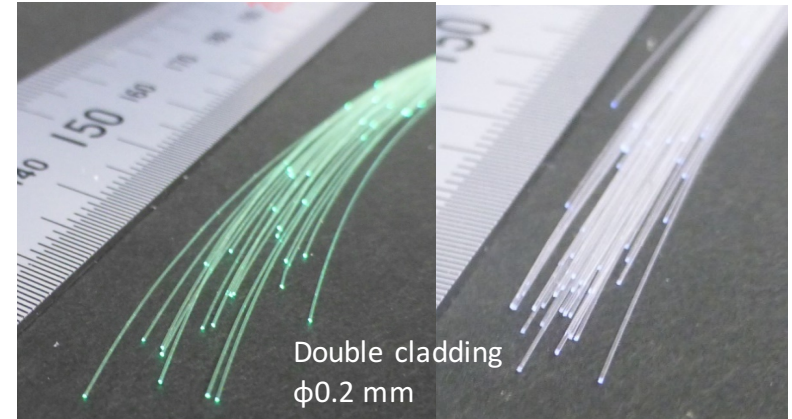
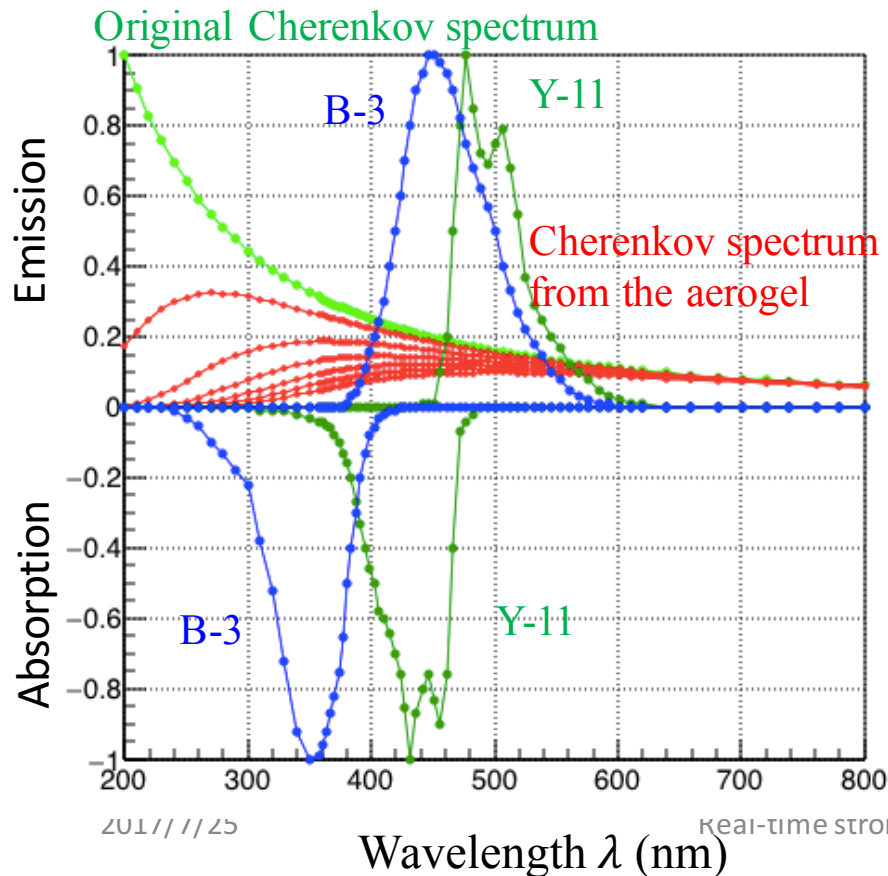


Double cladding

## 2. Basic concept an aerogel Cherenkov detector using wavelength-shifting fibers

Optical models

Wavelength-shifting fibers



Kuraray Y-11(300)MJ

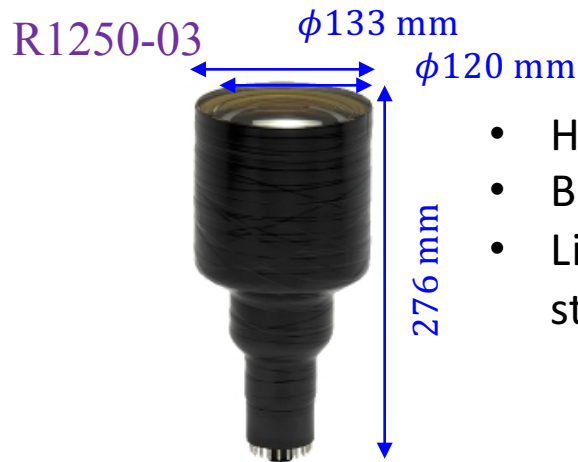
B-3(300)MJ

- Absorption spectra have peaks at 350 nm (B-3) and 450 nm (Y-11).
- Use of two types of fibers allows to extend wavelength range to absorb Cherenkov photons.

## 2. Basic concept an aerogel Cherenkov detector using wavelength-shifting fibers

Optical models

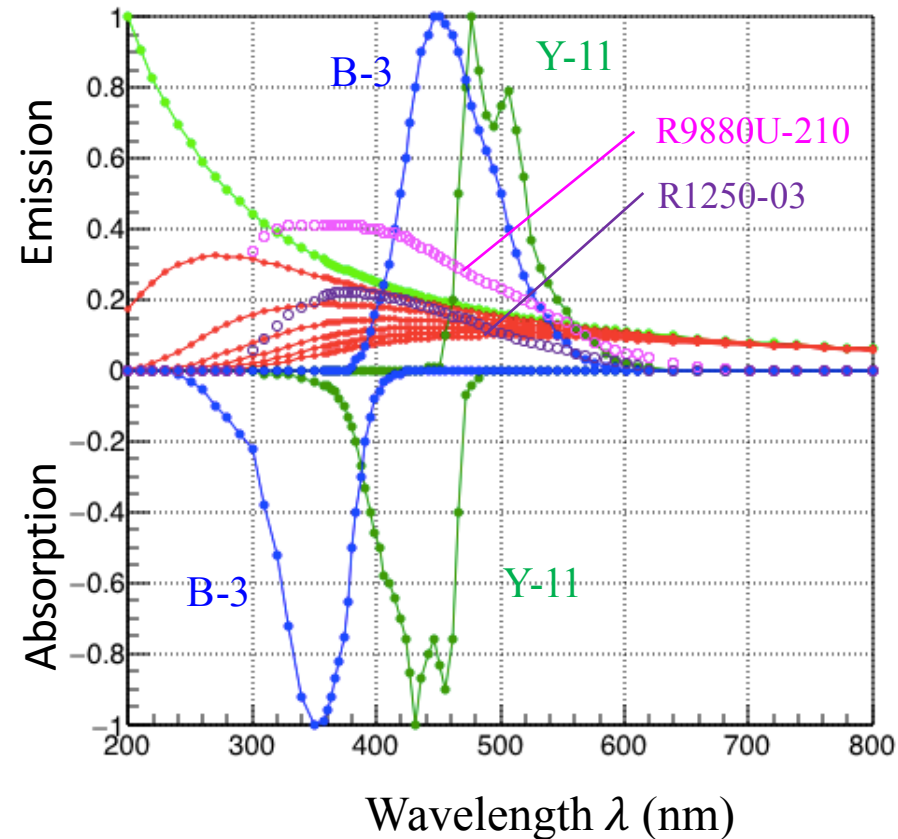
PMT



- Head-on Type
- Bi-alkali photocathode
- Line focused dynode structure

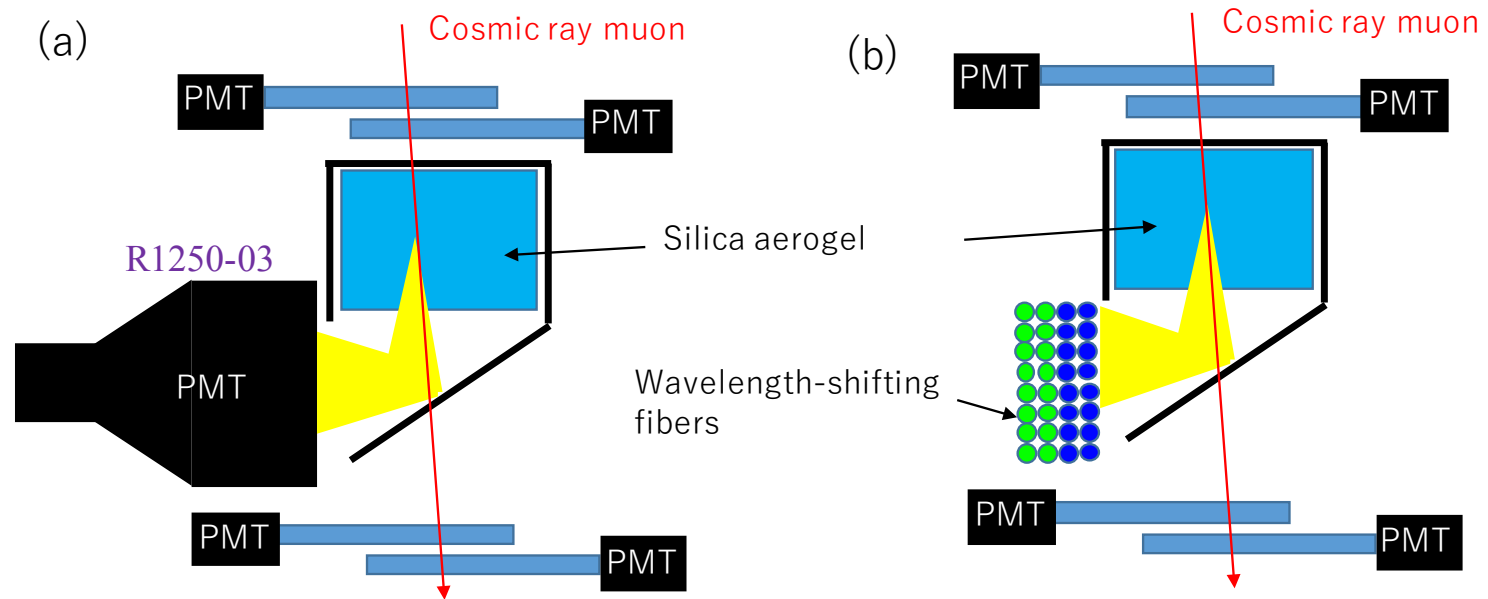


- Head-on Type
- Ultra Bi-alkali photocathode
- Metal channel dynode structure



## 2. Basic concept an aerogel Cherenkov detector using wavelength-shifting fibers

Measurement of light collection efficiency



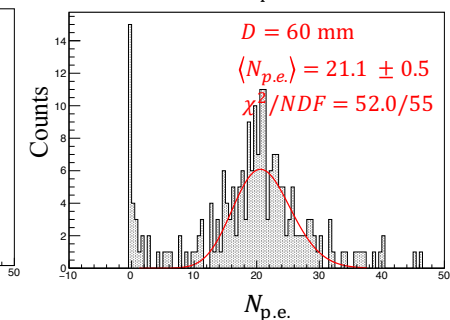
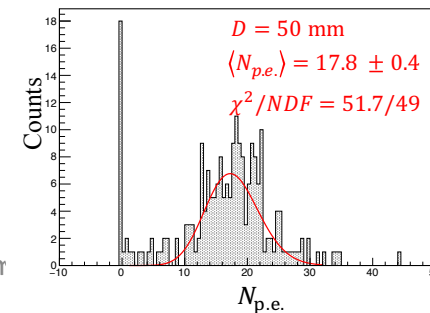
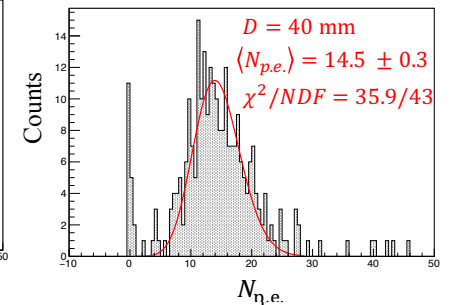
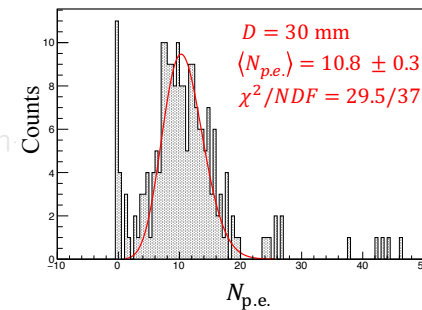
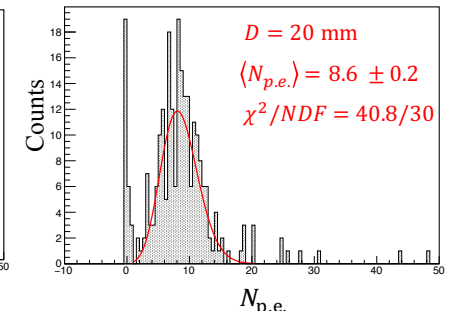
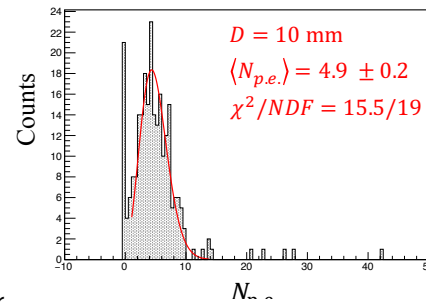
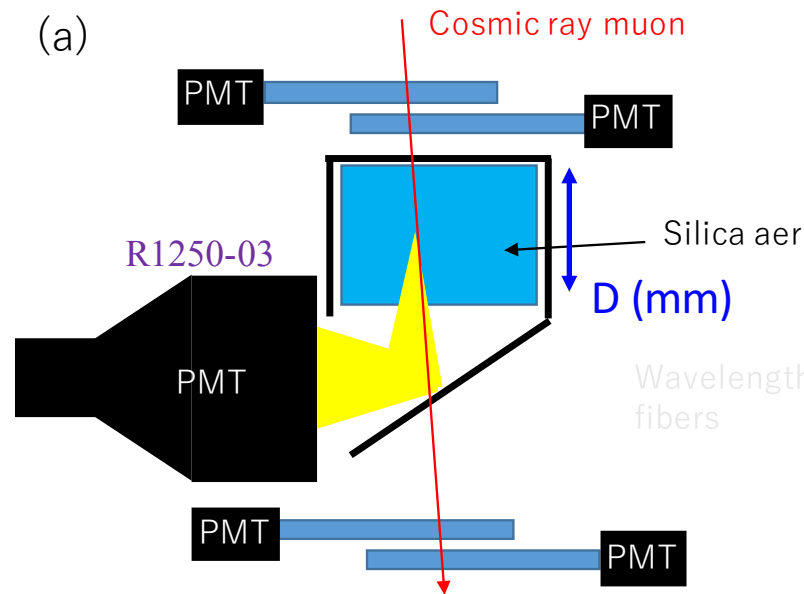
## 2. Basic concept an aerogel Cherenkov detector using wavelength-shifting fibers

Measurement of light collection efficiency

Poisson Function Fitting

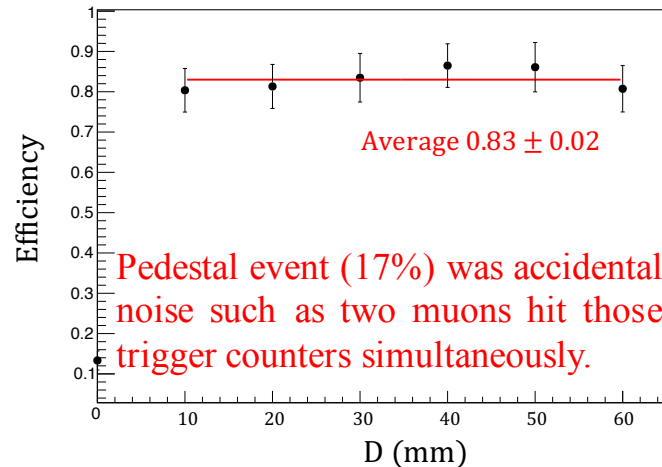
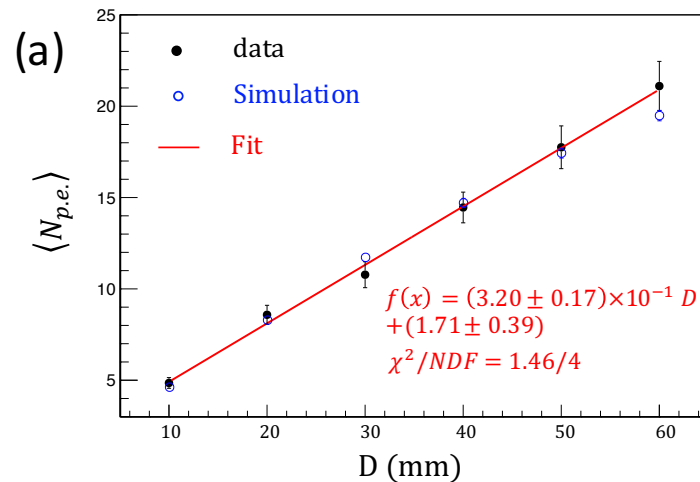
$$P(k, \nu) = e^{-\nu} \nu^k / k!$$

$$\langle N_{p.e.} \rangle (= \nu)$$



## 2. Basic concept an aerogel Cherenkov detector using wavelength-shifting fibers

Measurement of light collection efficiency



$$N_{p.e.} = 2\pi\alpha \int d\lambda dL \frac{\varepsilon_{QE}(\lambda) \cdot T(\lambda, L) \cdot \varepsilon_{ref}}{\lambda^2} + N_0$$

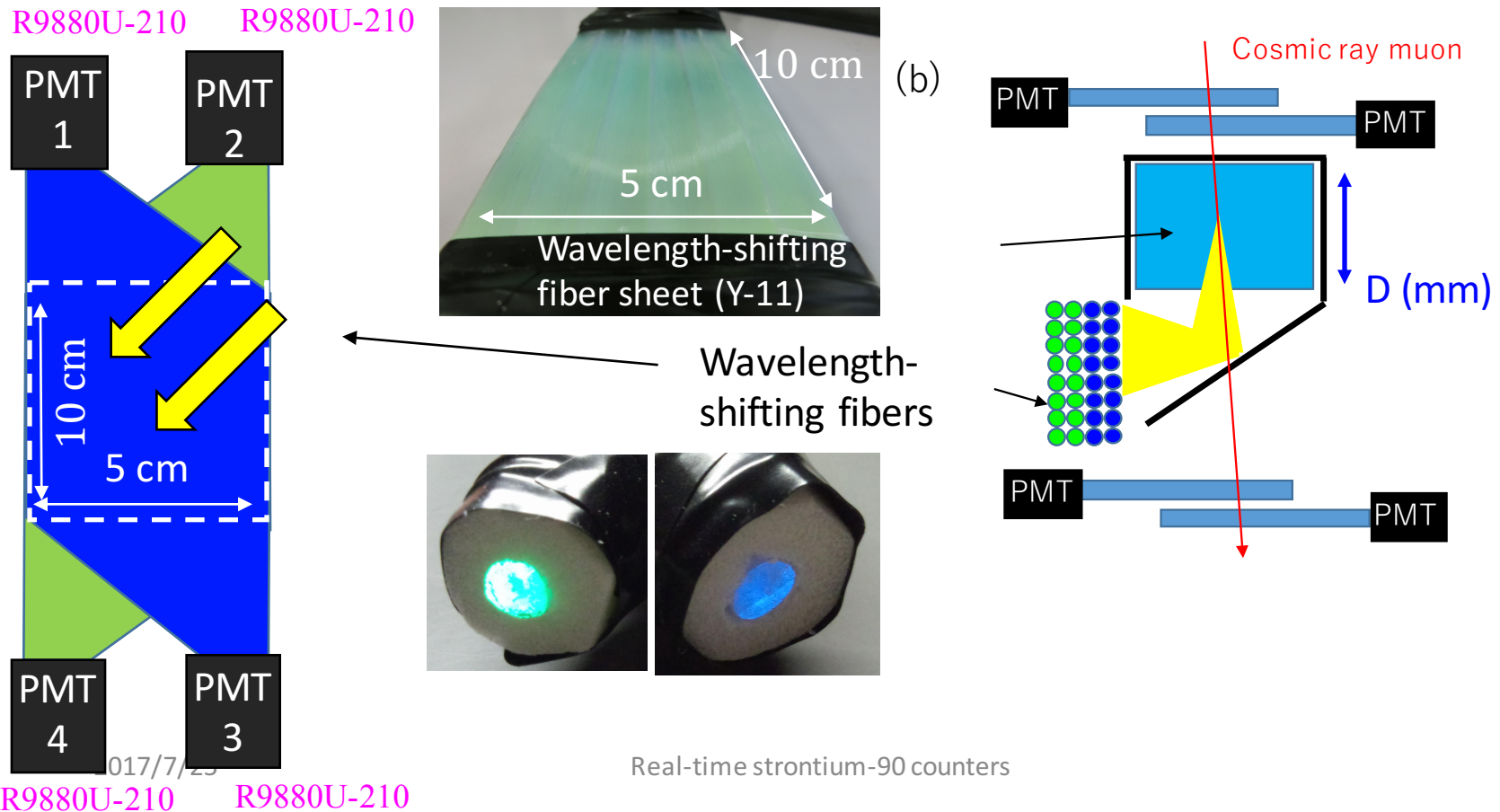
$$\varepsilon_{ref} = 0.466 \pm 0.004$$

$$N_0 = 1.42 \pm 0.03$$

$$\text{with } \chi_{min}^2 = 30.7$$

## 2. Basic concept an aerogel Cherenkov detector using wavelength-shifting fibers

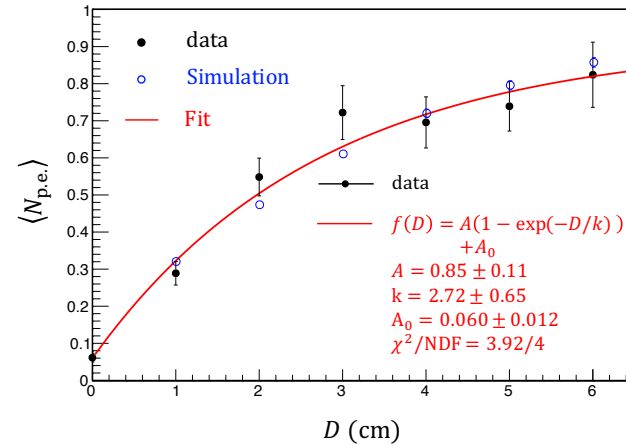
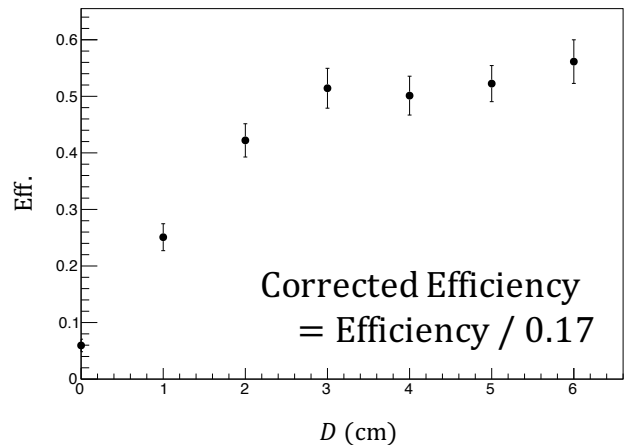
Measurement of light collection efficiency



## 2. Basic concept an aerogel Cherenkov detector using wavelength-shifting fibers

Measurement of light collection efficiency

(b)



$$P(k = 0, \nu) = \exp(-\nu)$$

$$\langle N_{\text{p.e.}} \rangle \equiv \nu = -\ln(\text{inefficiency})$$

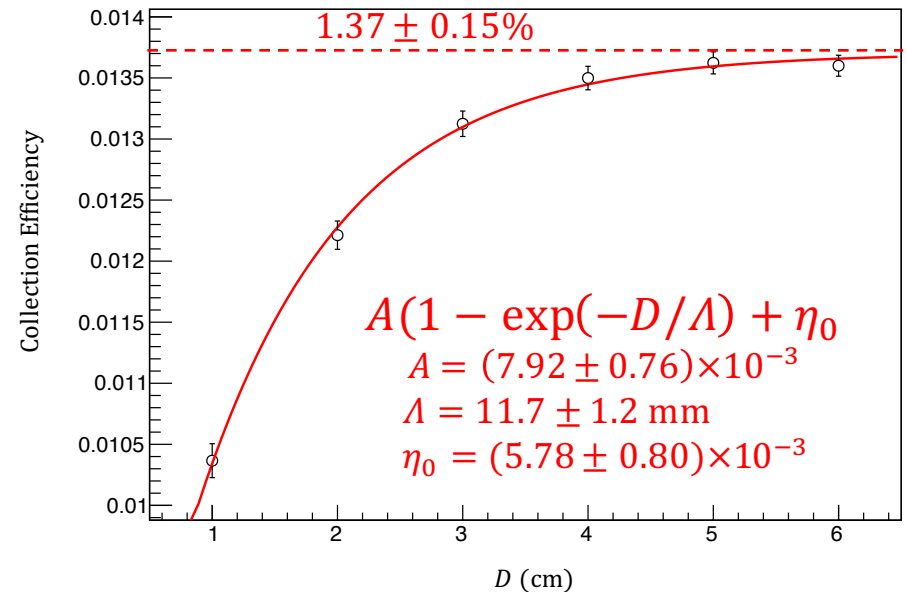
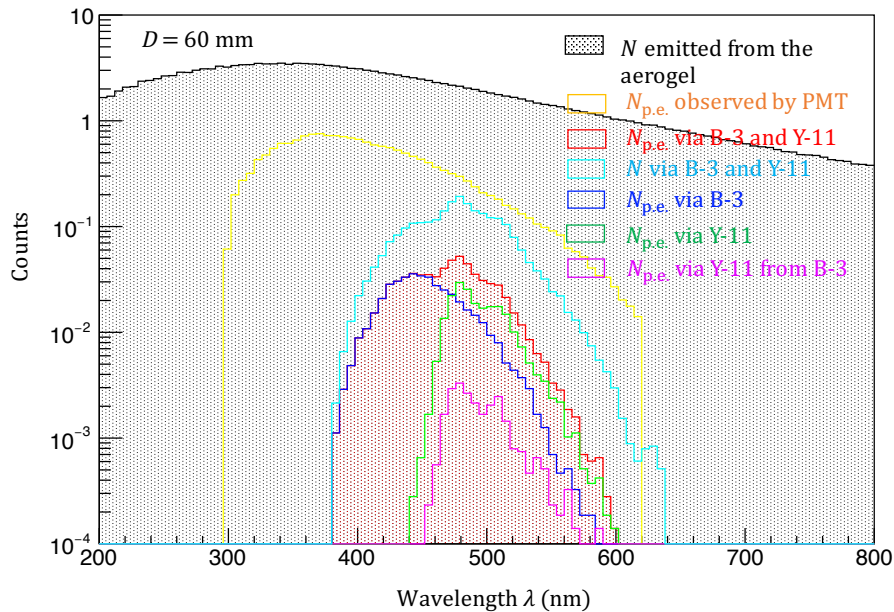
$$\begin{aligned}
 N_{\text{p.e.}} = & 2\pi\alpha \int d\lambda dL \frac{T(\lambda, L) \cdot \varepsilon_{\text{ref}}}{\lambda^2} \\
 & \left\{ \begin{aligned}
 & g_{\text{core}}^{\text{B-3}}(\lambda, \lambda') \varepsilon_{\text{trap}} \varepsilon_{\text{QE}}(\lambda') d\lambda' \\
 & + \frac{1}{2} g_{\text{core}}^{\text{B-3}}(\lambda, \lambda') g_{\text{core}}^{\text{Y-11}}(\lambda', \lambda'') (1 - \varepsilon_{\text{trap}}) \varepsilon_{\text{trap}} \varepsilon_{\text{QE}}(\lambda'') d\lambda'' \\
 & + (1 - g_{\text{core}}^{\text{B-3}}) g_{\text{core}}^{\text{Y-11}}(\lambda, \lambda'') \varepsilon_{\text{trap}} \varepsilon_{\text{QE}}(\lambda'') d\lambda'' \end{aligned} \right\} \\
 & + N_0,
 \end{aligned}$$



## 2. Basic concept an aerogel Cherenkov detector using wavelength-shifting fibers

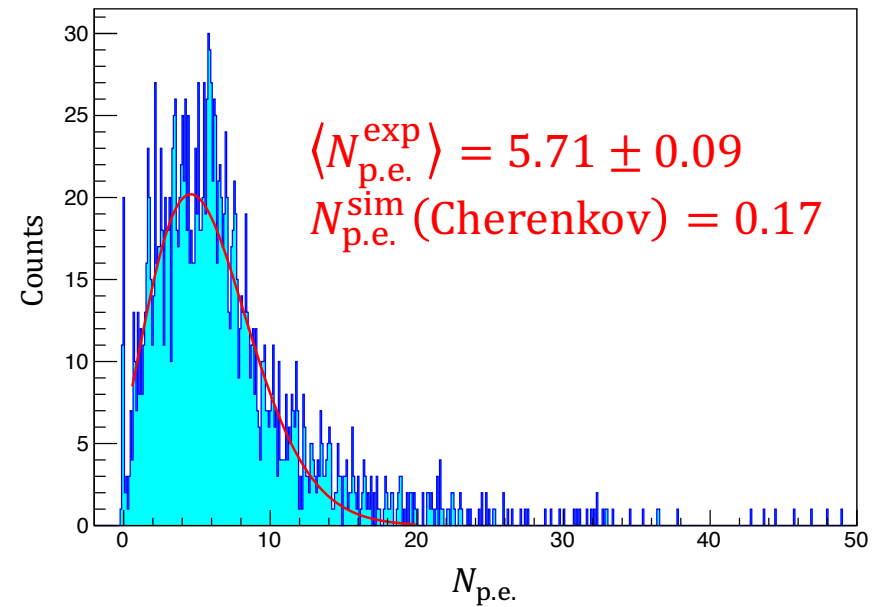
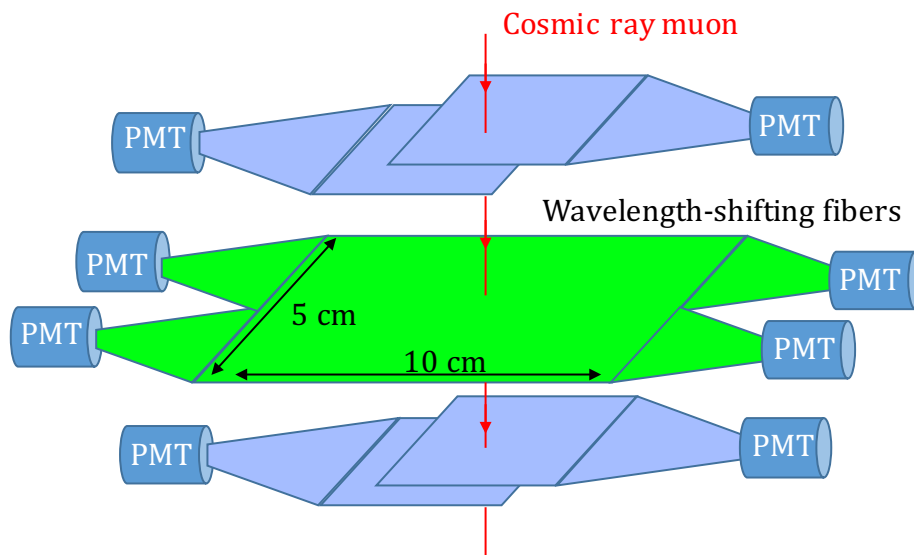
Measurement of light collection efficiency

(b)



## 2. Basic concept an aerogel Cherenkov detector using wavelength-shifting fibers

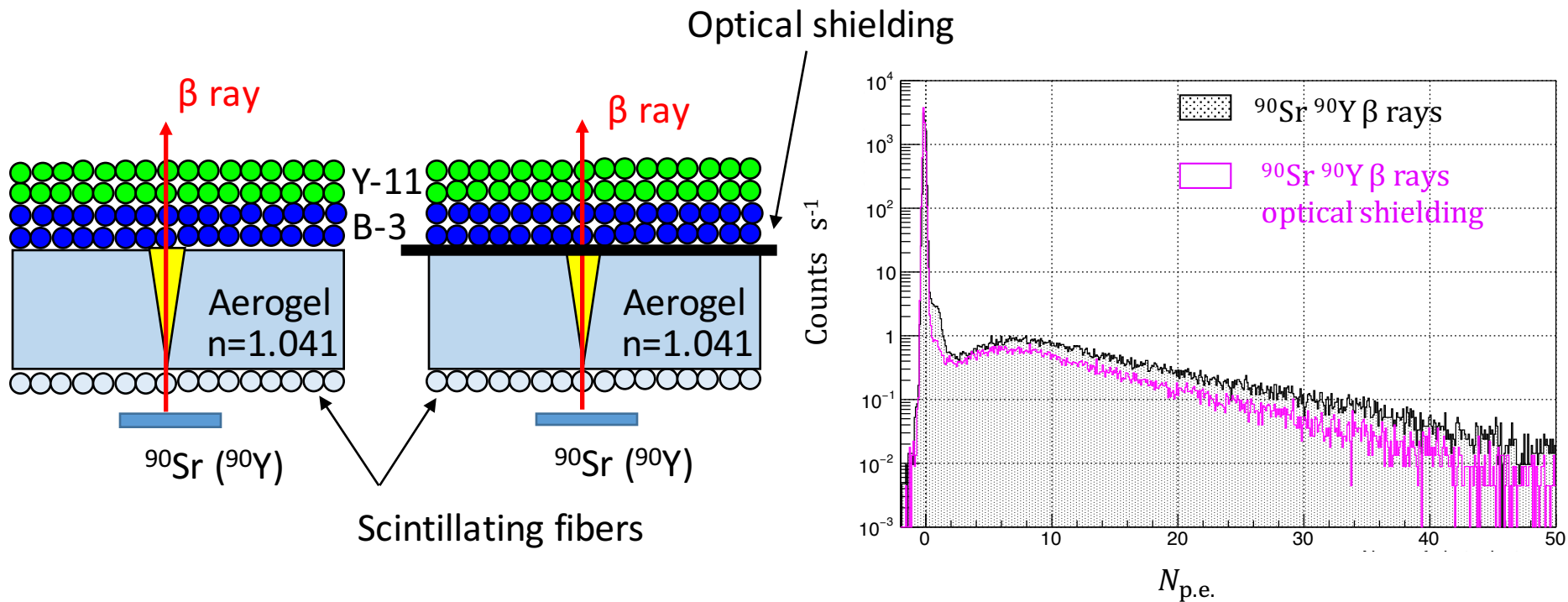
Impact of charged particles passing through the fibers



It was considered that wavelength-shifting fiber has a property of scintillation radiation.

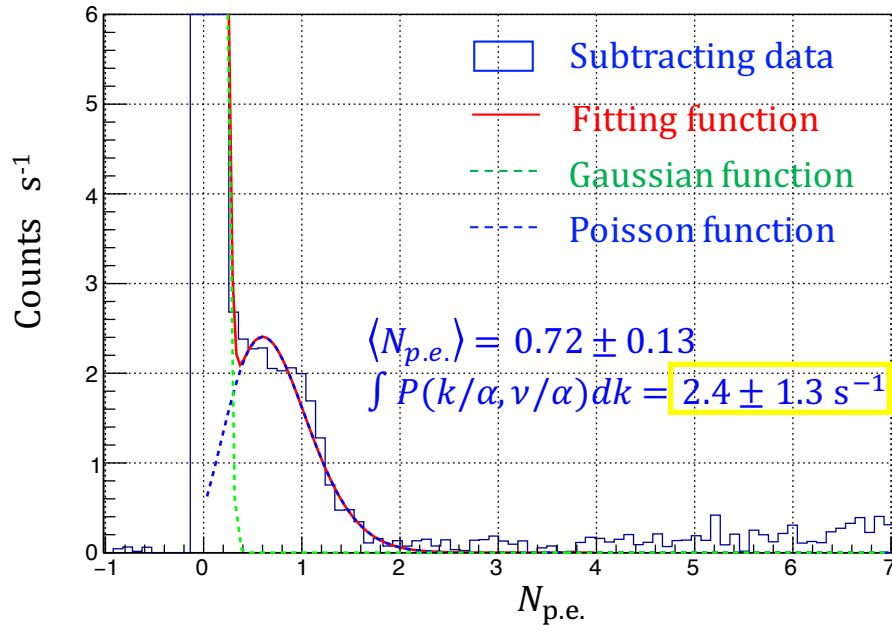
## 2. Basic concept an aerogel Cherenkov detector using wavelength-shifting fibers

Cherenkov photons from  $^{90}\text{Sr}$  and  $^{90}\text{Y}$   $\beta$  rays



## 2. Basic concept an aerogel Cherenkov detector using wavelength-shifting fibers

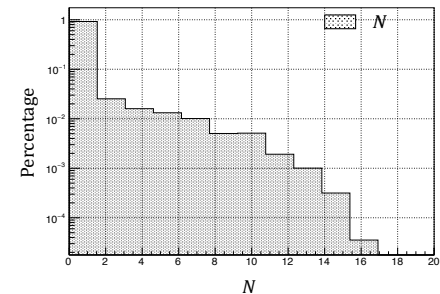
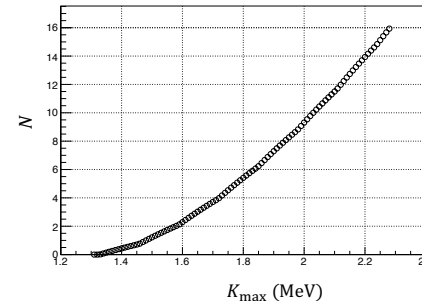
Cherenkov photons from  $^{90}\text{Sr}$  and  $^{90}\text{Y}$   $\beta$  rays



Count rate

$$\begin{aligned}
 &= A_{\text{Sr+Y}} \cdot \Omega \cdot \eta \\
 &= 2 \times 23.6 \text{ kBq} \cdot 0.099 \cdot 5.04 \times 10^{-4} \\
 &= 2.35 \text{ s}^{-1},
 \end{aligned}$$

where  $\eta = \int dN dN_{p.e.} \exp(-\delta(N)\varepsilon(N \rightarrow N_{p.e.}))$



## 2. Basic concept an aerogel Cherenkov detector using wavelength-shifting fibers

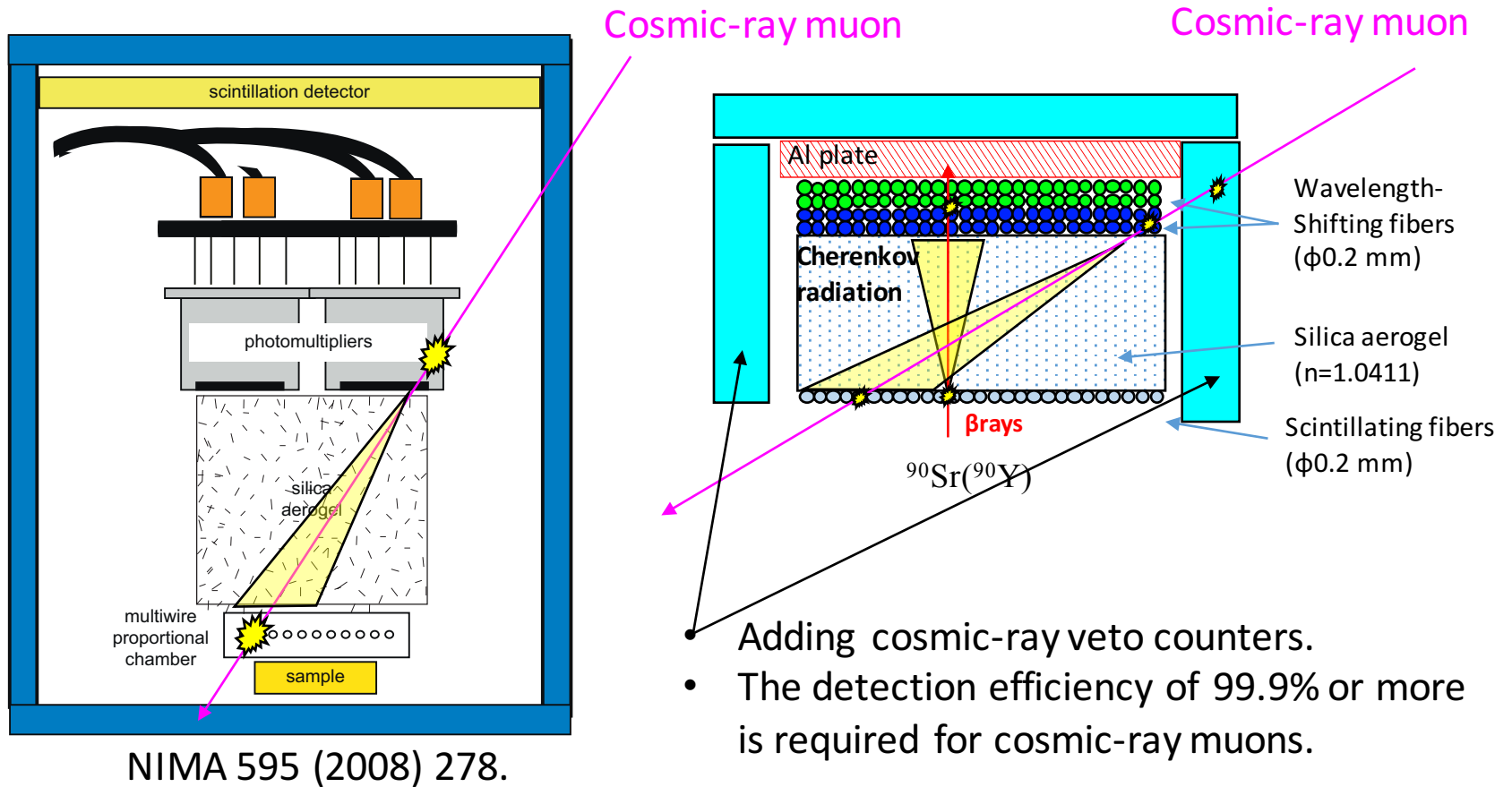
### Results

- Aerogel ( $n=1.0411$ ):  $K_{th}=1.31$  MeV,  $E_{\gamma}^{(thr.)}=1.53$  MeV.
- Accidental noise can be reduce to 11% using the fibers than 5-sinch PMT reading.
- Optical models were developed for the Cherenkov detector.
  1. Cherenkov spectrum
  2. Silica aerogel transmittance
  3. Wavelength-shifting fibers absorption & emission spectrum
  4. PMT quantum efficiency
  5. Fix with cosmic-ray test
- Light collection efficiency was determined to be 1.0-1.4%.
- Cherenkov photons by  $^{90}\text{Y}$   $\beta$  rays were observed using the aerogel and B-3 & Y-11.

### 3. Background study of environmental radiation

### 3. Background study of environmental radiation

#### 3.1. Cosmic-ray muons



### 3. Background study of environmental radiation

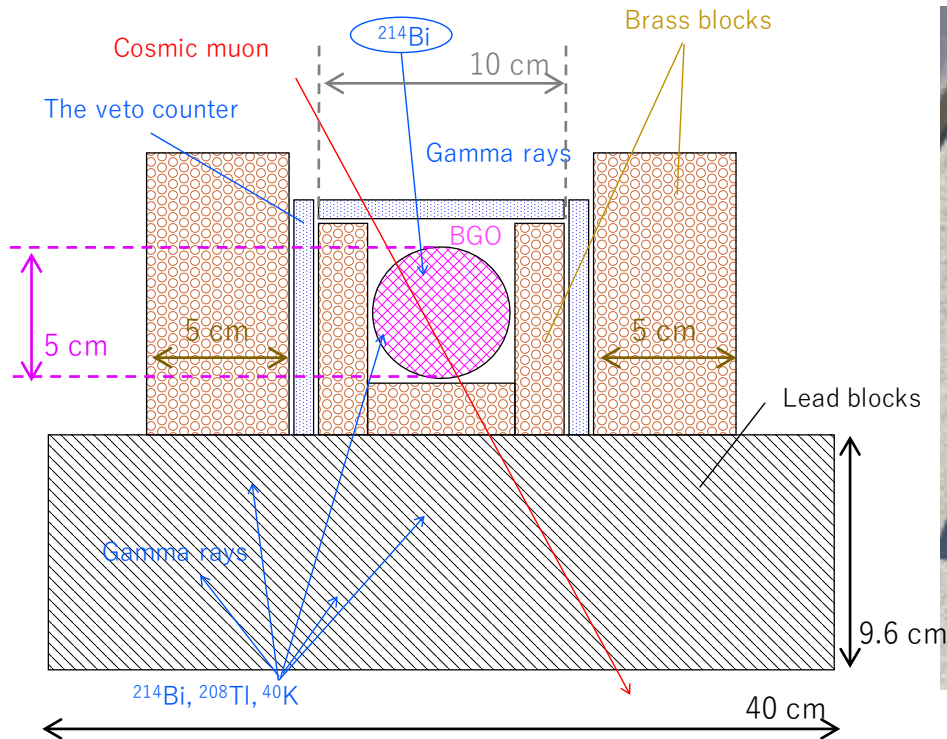
#### 3.2. $\gamma$ -rays energy spectroscopy of the air

- It was considered that  $^{40}\text{K}$  is not to be background because knocked out  $e^-$  from  $\gamma$  ray (1.46 MeV) dose not satisfy the Cherenkov condition in the aerogel ( $n=1.041$ ).
- Thorium include in the concrete blocks of the buildings. Radon progenies attach on surface in the environmental.
- Knocked out  $e^-$  from  $\gamma$  rays ( $E_\gamma > 1.53$  MeV) emitted from  $^{214}\text{Bi}$  and  $^{208}\text{Tl}$  can satisfy the Cherenkov condition there.
- Average of radon ( $^{222}\text{Rn}$ ) concentration in the air is  $45 \text{ Bq/m}^3$ .
- Here, radon progenies (particularly  $^{214}\text{Bi}$ ) in the air were focused by the study.
- $^{214}\text{Bi}$  emits  $\beta$  rays (max. 3.27 MeV).



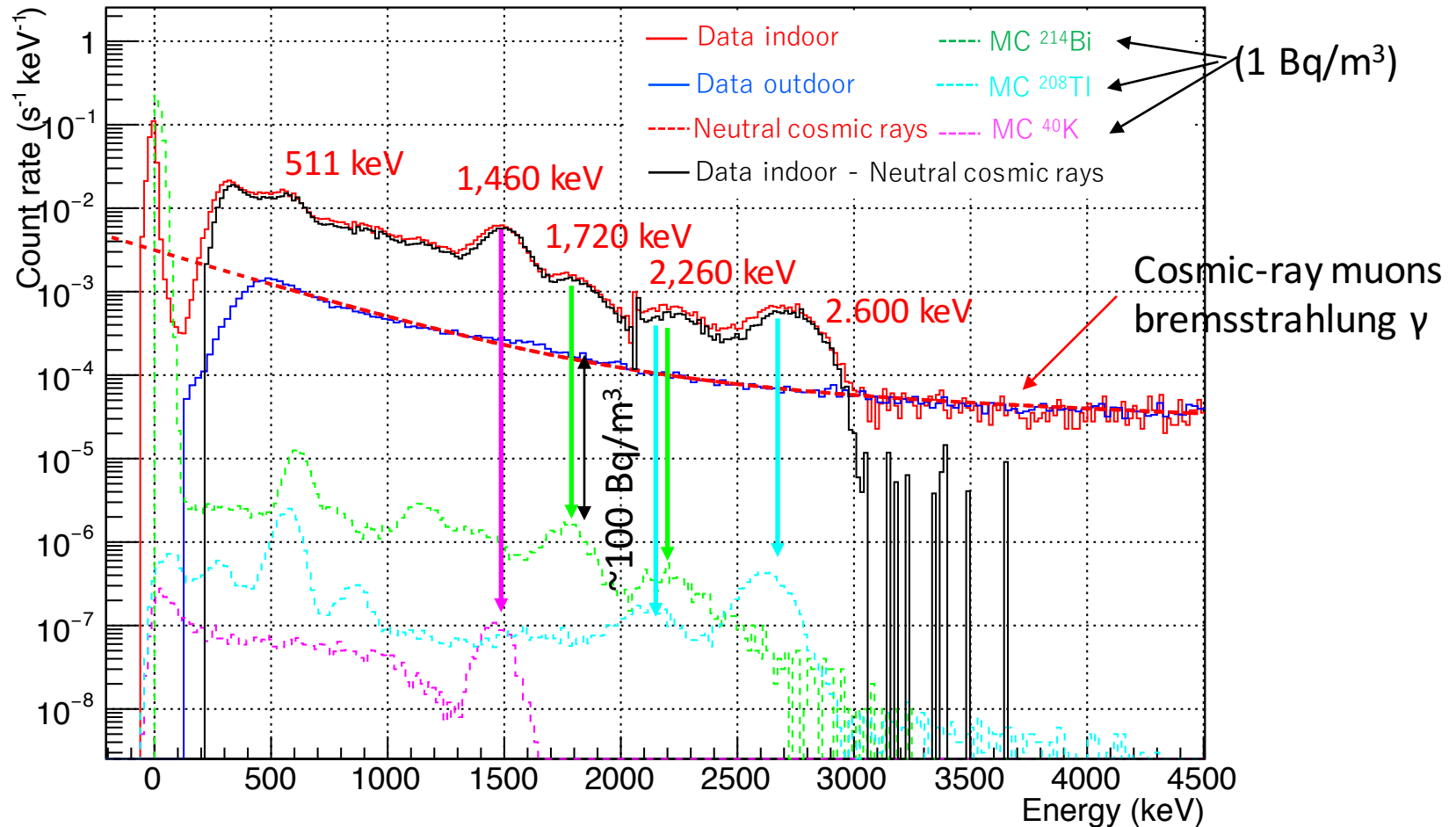
### 3. Background study of environmental radiation

#### 3.2. $\gamma$ -rays energy spectroscopy of the air



### 3. Background study of environmental radiation

#### 3.2. $\gamma$ -rays energy spectroscopy of the air



## 3. Background study of environmental radiation

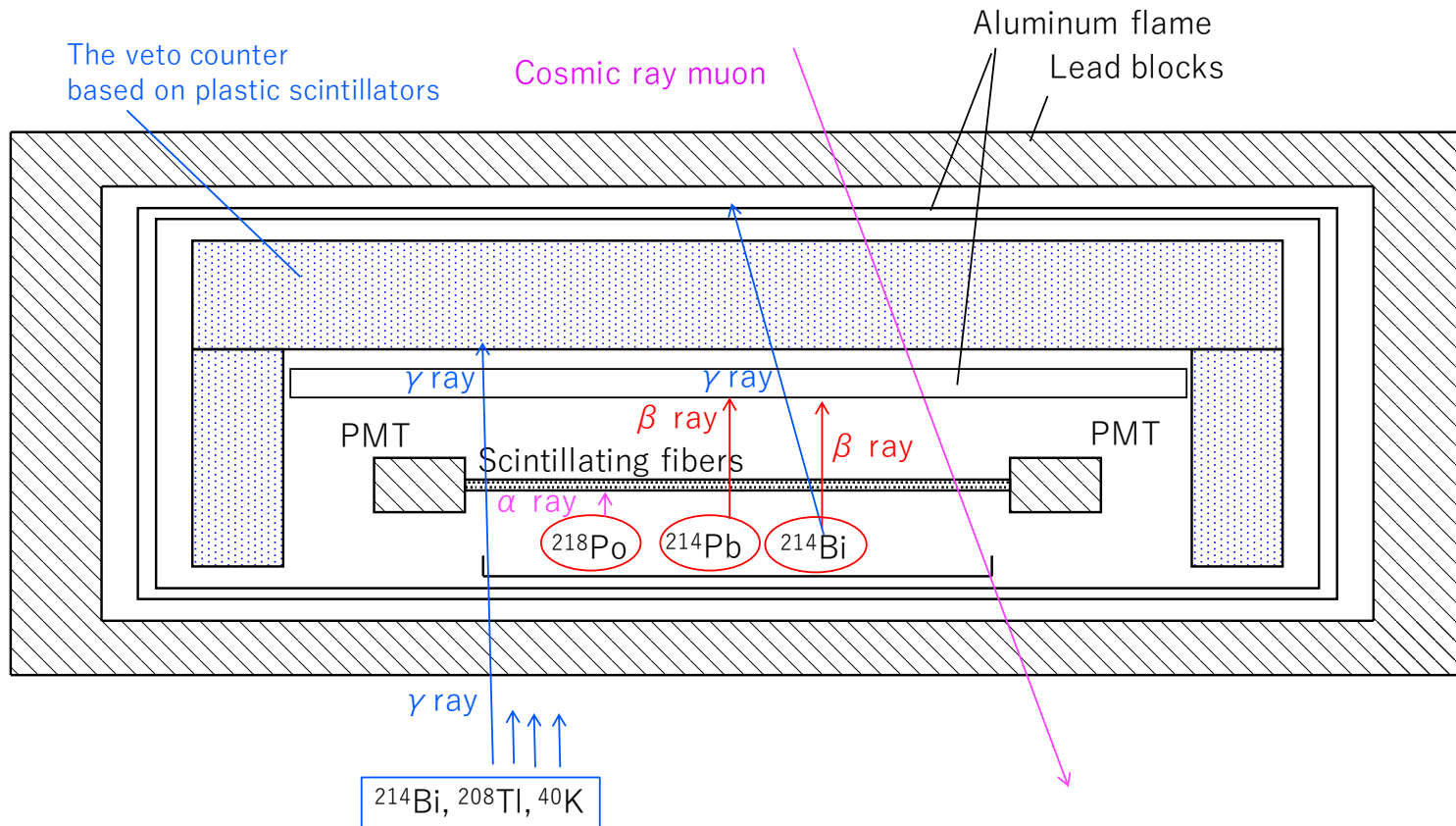
### 3.2. $\gamma$ -rays energy spectroscopy of the air

#### Results

- $^{214}\text{Bi}$  concentration in the air is less than  $100 \text{ Bq/m}^3$ .
- Gap between sample and trigger counter should be less than 1 cm.
- The air in space under the sample should be removed out.

### 3. Background study of environmental radiation

#### 3.3. $\beta$ rays surface inspection of sample sheets adsorbing radon progenies



### 3. Background study of e

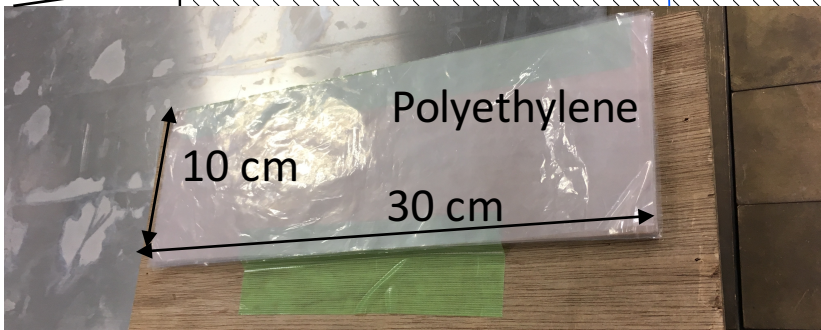
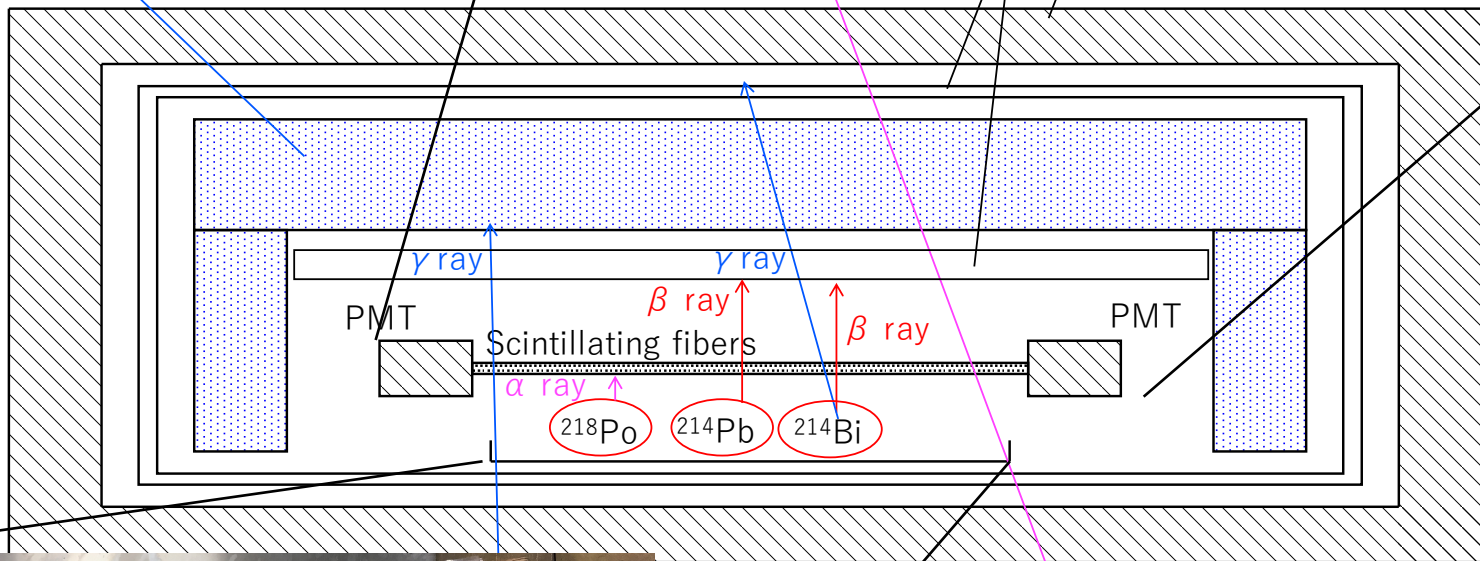
#### 3.3. $\beta$ rays surface inspection of sa



The veto counter based on plastic scintillators

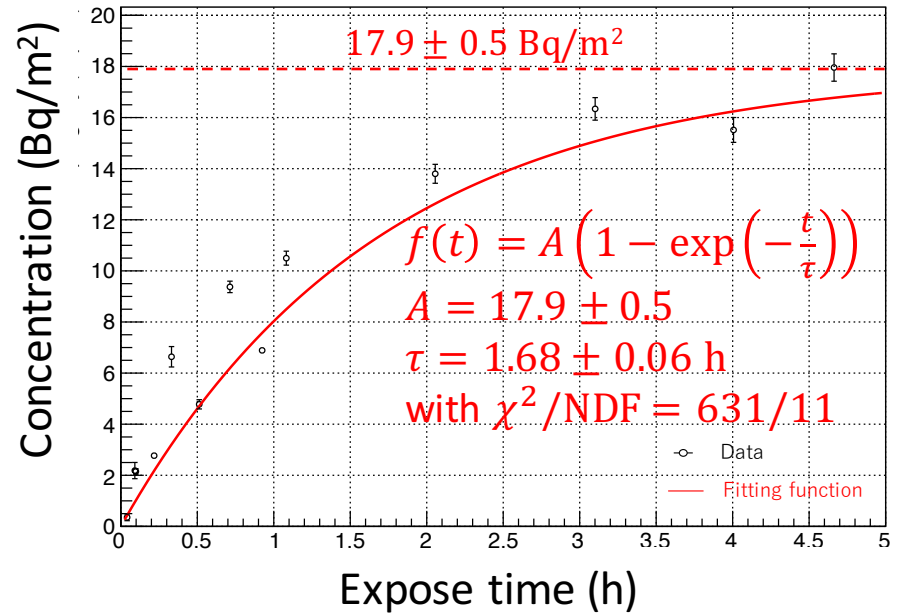
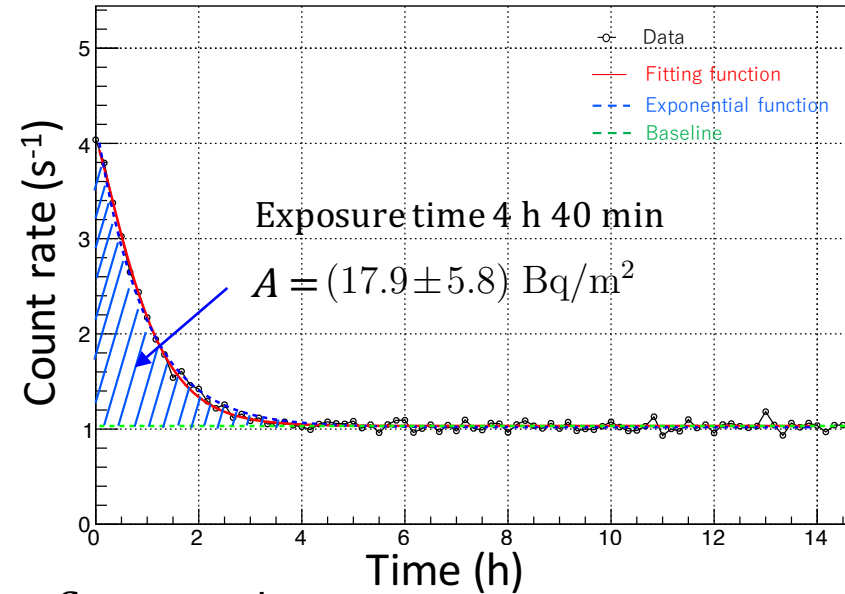
Cosmic ray muon

Aluminum frame  
Lead blocks



### 3. Background study of environmental radiation

#### 3.3. $\beta$ rays surface inspection of sample sheets adsorbing radon progenies



Concentration

$$A = \sum_j (C(t_j) - R_{\text{BG}}) \Delta t_j \frac{\eta_\varepsilon k_\rho}{\varepsilon_{\text{Sr}} S}$$

$C(t_j)$ : counting rate

$R_{\text{BG}}$ : background rate

$\Delta t = 10 \text{ min}$

$\varepsilon_{\text{Sr}}$ :  $^{90}\text{Sr}$  eff. =  $(8.68 \pm 0.01) \times 10^2 \text{ Bq}^{-1} \text{ h}^{-1}$

$\eta_\varepsilon$ : ratio of  $^{90}\text{Sr}$  eff. to radon prog. eff. = 0.37

$k_\rho$ : correction coefficient = 1.15

$S$ :  $0.03 \text{ m}^2$

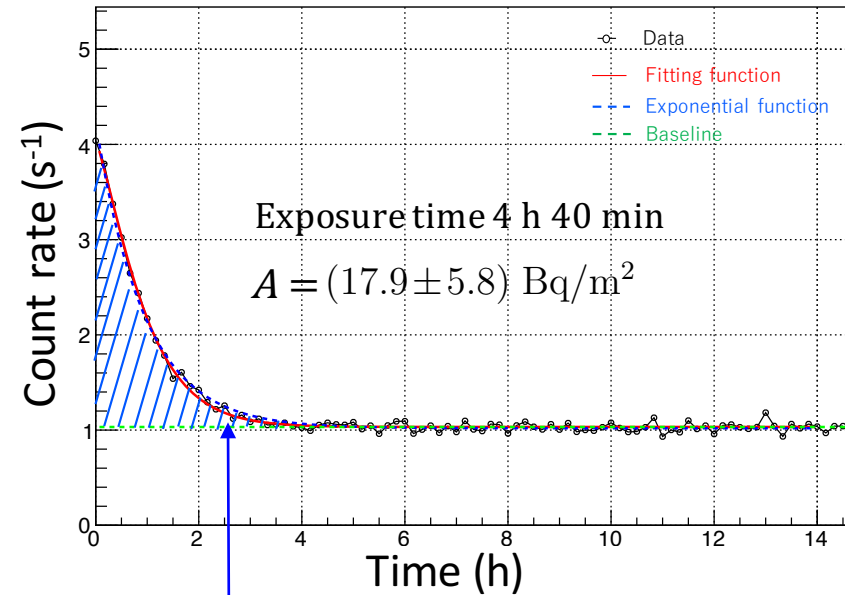
real-time stro

Interpretation

- (1)  $^{218}\text{Po}$  only falls on the sample after the radon decay in the air.  $^{214}\text{Pb}$  and  $^{214}\text{Bi}$  produced at the sample.
- (2)  $^{218}\text{Po}$ ,  $^{214}\text{Pb}$ , and  $^{214}\text{Bi}$  in the air fall the sample after the radon decay in the air.

### 3. Background study of environmental radiation

#### 3.3. $\beta$ rays surface inspection of sample sheets adsorbing radon progenies



Simple exponential function fit

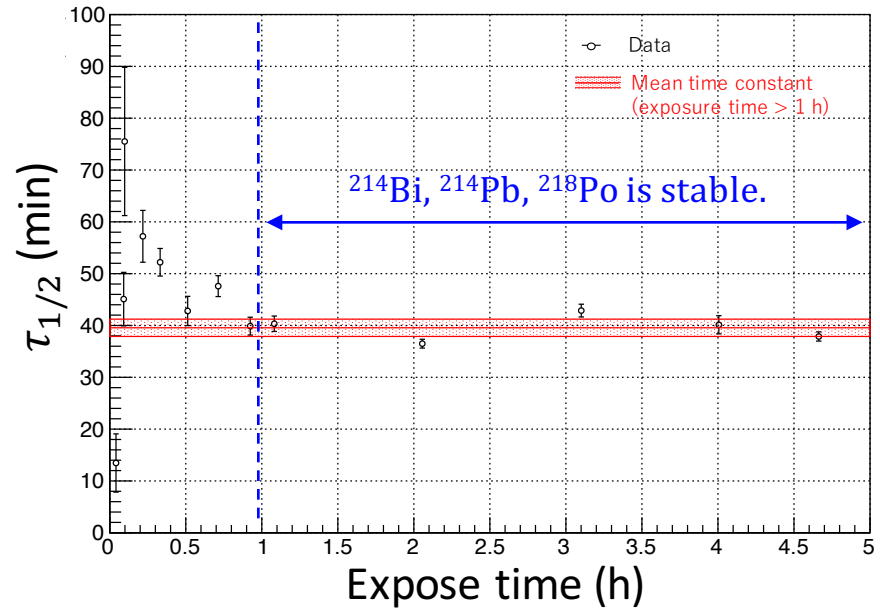
$$f(t) = A \exp(-t \ln 2 / \tau_{1/2}) + R_{BG}$$

$$A = 3.22 \pm 0.04$$

$$\tau_{1/2} = (0.95 \pm 0.02) \text{ h}$$

$$R_{BG} = (1.02 \pm 0.01) \text{ s}^{-1}$$

$$\text{with } \chi^2 / \text{NDF} = 0.32 / 69$$

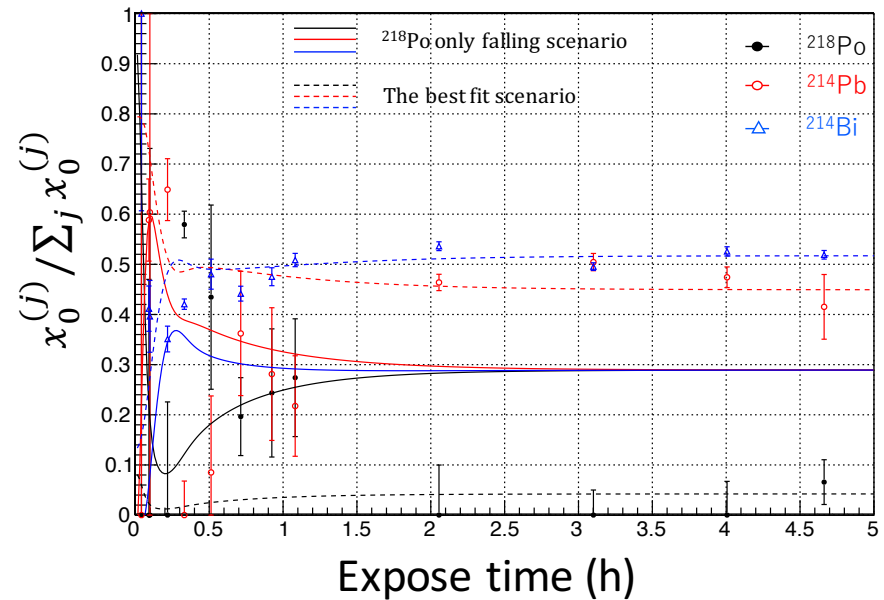
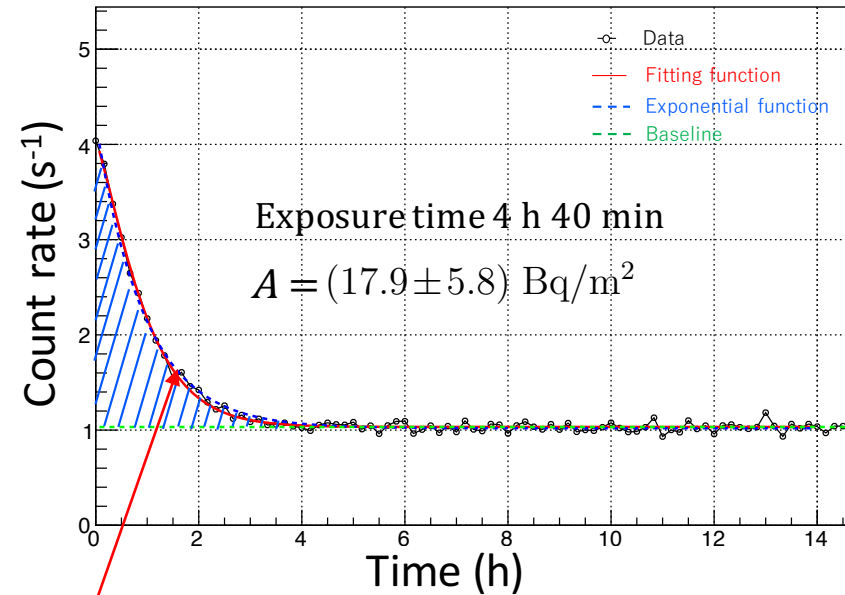


Interpretation

- (1)  $^{218}\text{Po}$  only falls on the sample after the radon decay in the air.  $^{214}\text{Pb}$  and  $^{214}\text{Bi}$  produced at the sample.
- (2)  $^{218}\text{Po}$ ,  $^{214}\text{Pb}$ , and  $^{214}\text{Bi}$  in the air fall the sample after the radon decay in the air.

### 3. Background study of environmental radiation

#### 3.3. $\beta$ rays surface inspection of sample sheets adsorbing radon progenies



$$f(t) = \frac{\lambda_1 \lambda_2 x_0^{(1)}}{(\lambda_1 - \lambda_2)(\lambda_1 - \lambda_3)} \exp(-\lambda_1 t) + \left( \frac{\lambda_1 \lambda_2 x_0^{(1)}}{(\lambda_2 - \lambda_1)(\lambda_2 - \lambda_3)} + \frac{\lambda_2 x_0^{(2)}}{\lambda_3 - \lambda_2} \right) \exp(-\lambda_2 t) + \left( \frac{\lambda_1 \lambda_2 x_0^{(1)}}{(\lambda_2 - \lambda_1)(\lambda_2 - \lambda_3)} + \frac{\lambda_2 x_0^{(2)}}{\lambda_3 - \lambda_2} + x_0^{(3)} \right) \exp(-\lambda_3 t) + R_{BG},$$

free parameters

Isotope  $j = 1, 2, 3$  are  $^{218}\text{Po}$ ,  $^{214}\text{Pb}$ ,  $^{214}\text{Bi}$ , respectively.  
 $\lambda_j = \tau_j^{-1}$ : inverse of life time of isotope  $j$   
 $x_0^{(j)}$ : initial intensity of isotope  $j$   
 $R_{BG}$ : background rate



### 3. Background study of environmental radiation

#### 3.3. $\beta$ rays surface inspection of sample sheets adsorbing radon progenies

##### Result

- It was found that radon progenies of  $(17.9 \pm 0.5) \text{ Bq/m}^2$  were attached to the sample sheets.
- $^{214}\text{Bi}$  on the sample is not negligible, and it is required to not expose sample into the air.
- This result suggested to reject the scenario in the case of  $^{218}\text{Po}$  only falling on the sample after the radon decays in the air.
- Therefore, it is suggested that there are the radon progenies in the air Indirectly.
- The suggestion could be a clue for a search of the lung cancer occurring in non-smokers from the impact and exposures by inhalation of the radon progenies.

## 4. Design of a prototype detector

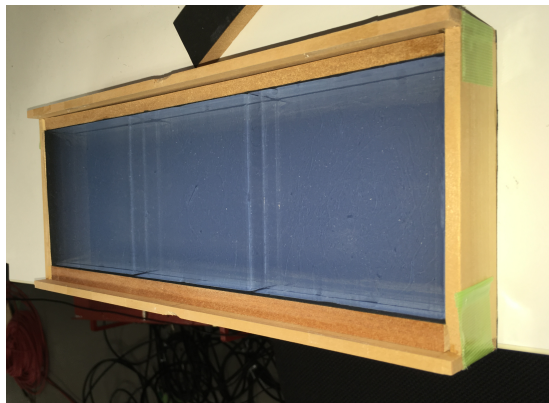
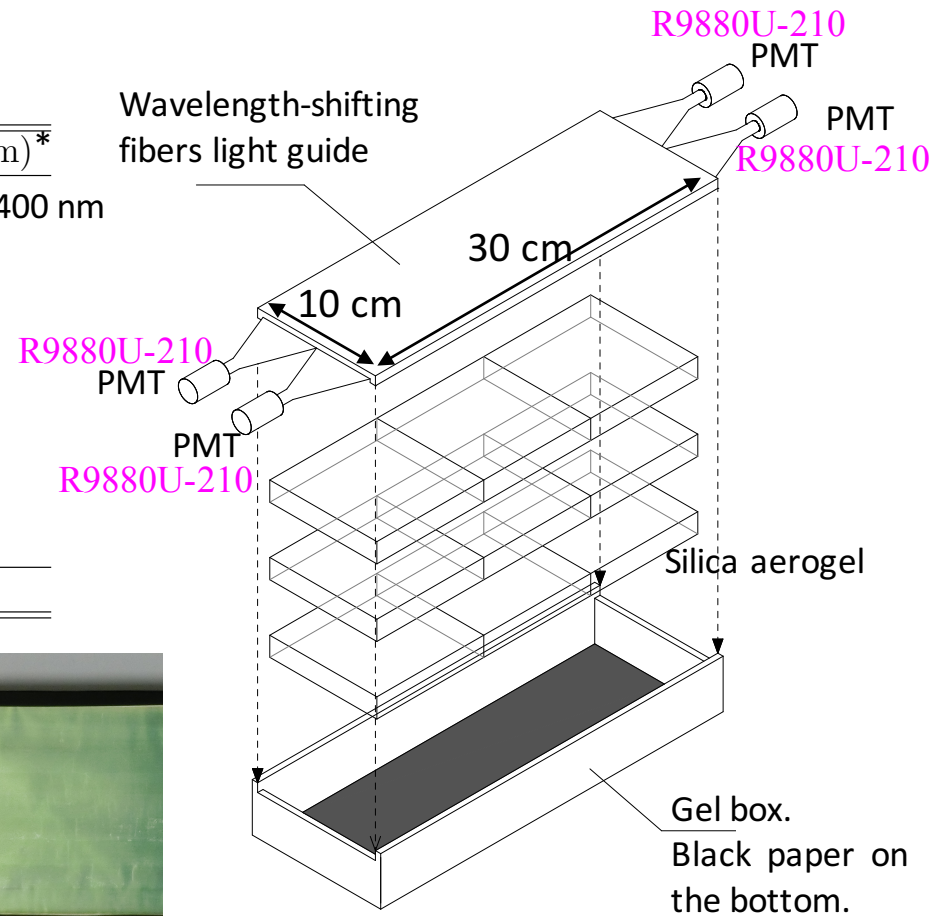
# 4. Design of a prototype detector

## 4.1. Threshold-type Cherenkov counter

Properties of the aerogel tiles

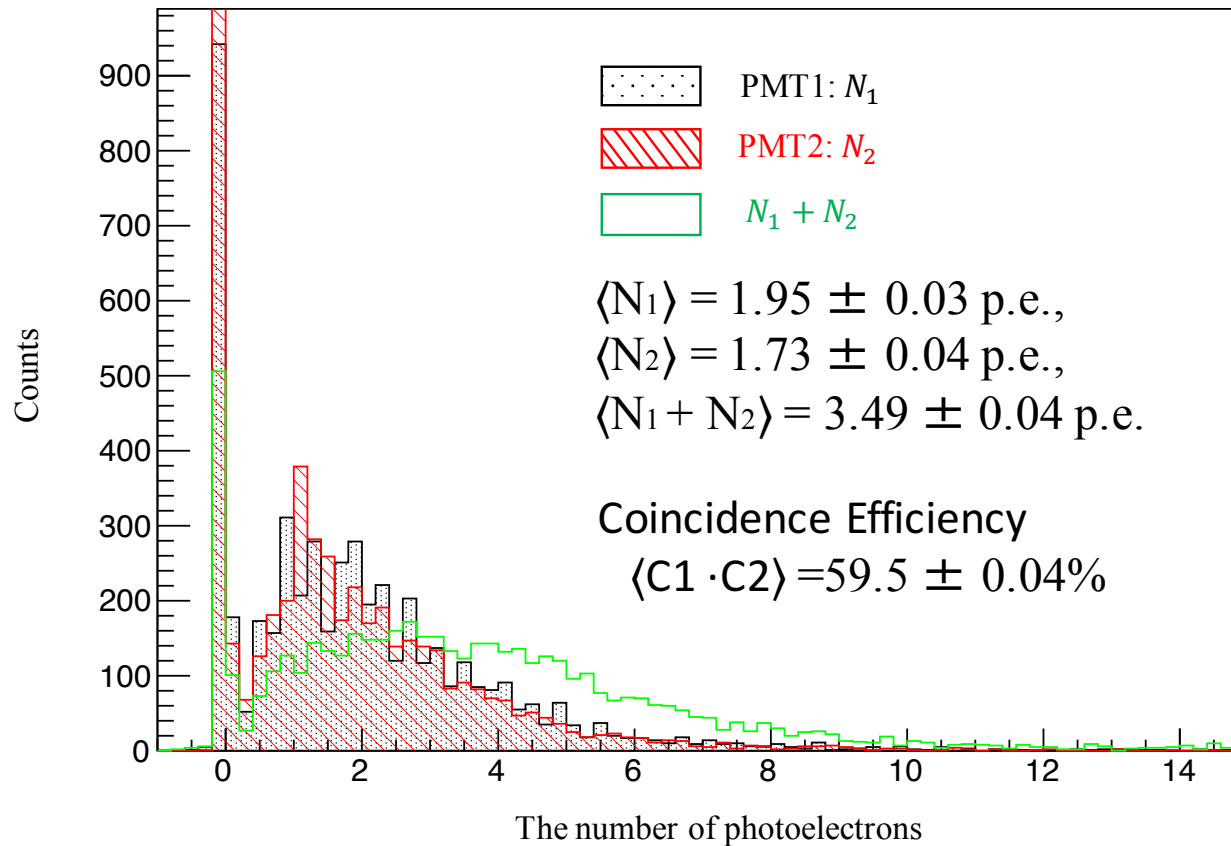
Tile	Refractive index	Transmission length (mm)*
MEC4-1a	1.0408	41.0
MEC4-1b	1.0411	38.6
MEC4-1c	1.0412	39.2
MEC4-2a	1.0414	40.9
MEC4-2b	1.0414	41.2
MEC4-2c	1.0414	41.7
MEC4-3a	1.0408	41.7
MEC4-3b	1.0410	41.4
MEC4-3c	1.0411	41.7
Mean	$1.0411 \pm 0.0002$	$40.8 \pm 1.1$

\* at 400 nm



# 4. Design of a prototype detector

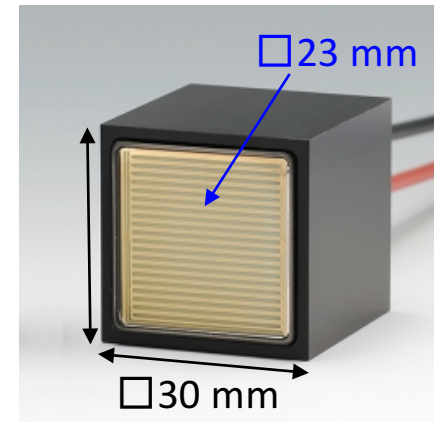
## 4.2. Trigger counter



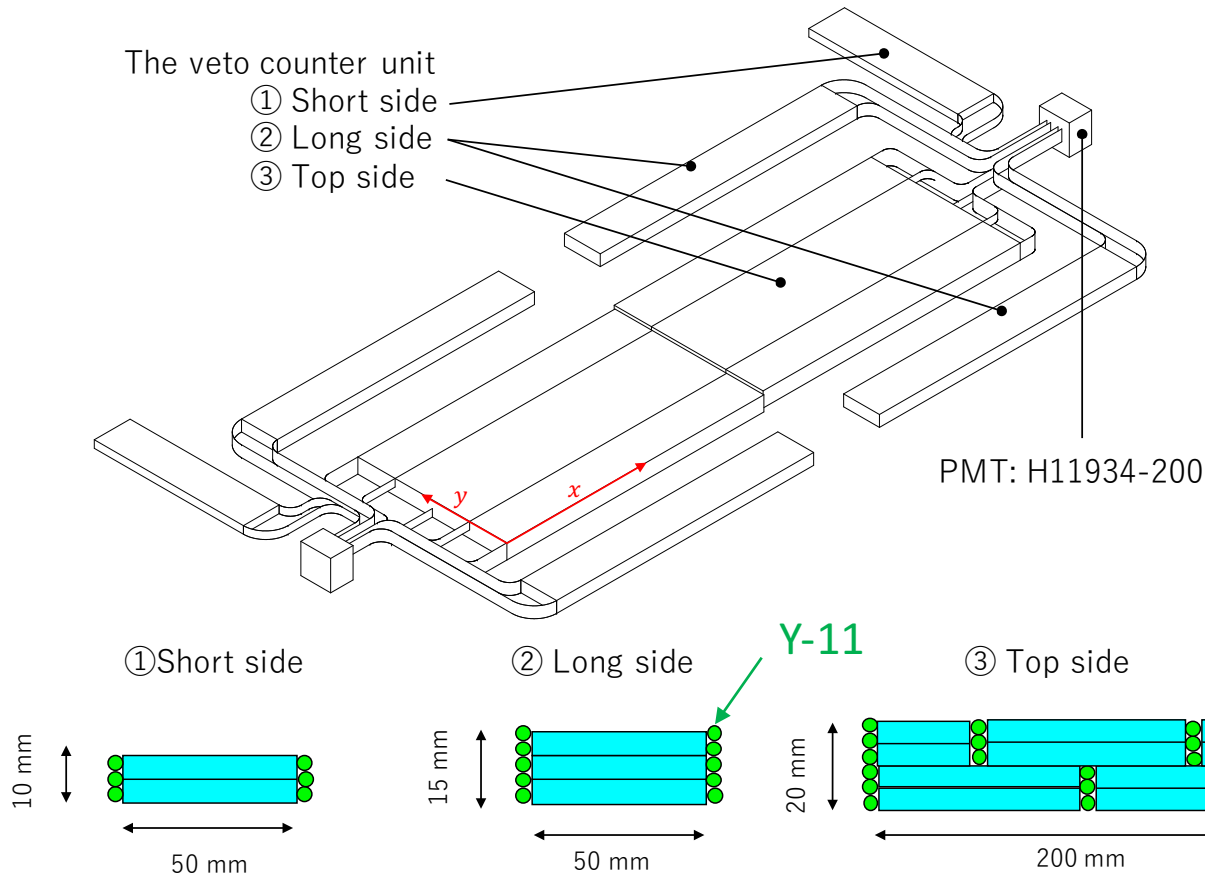
# 4. Design of a prototype detector

## 4.3. Veto counter

H11934-200

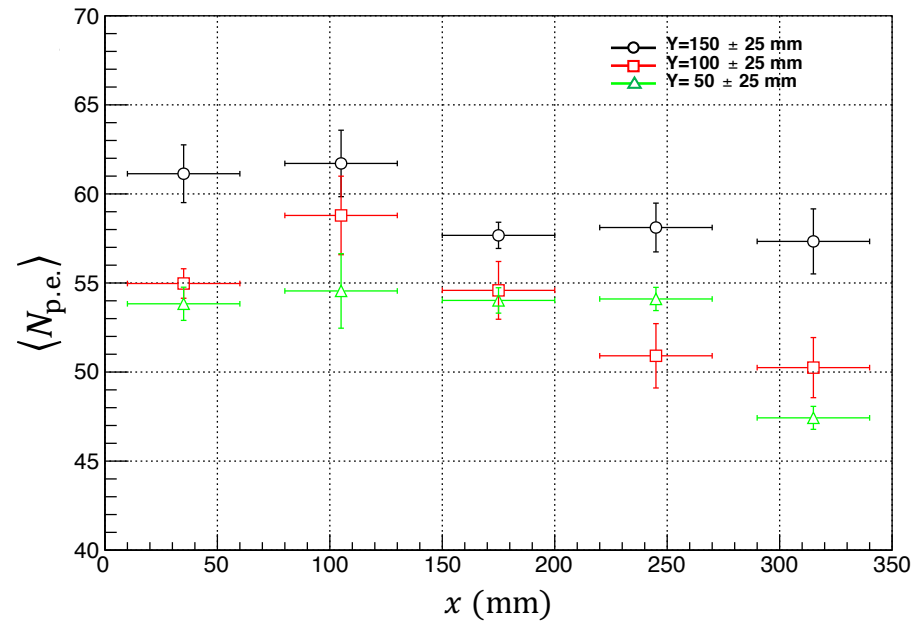
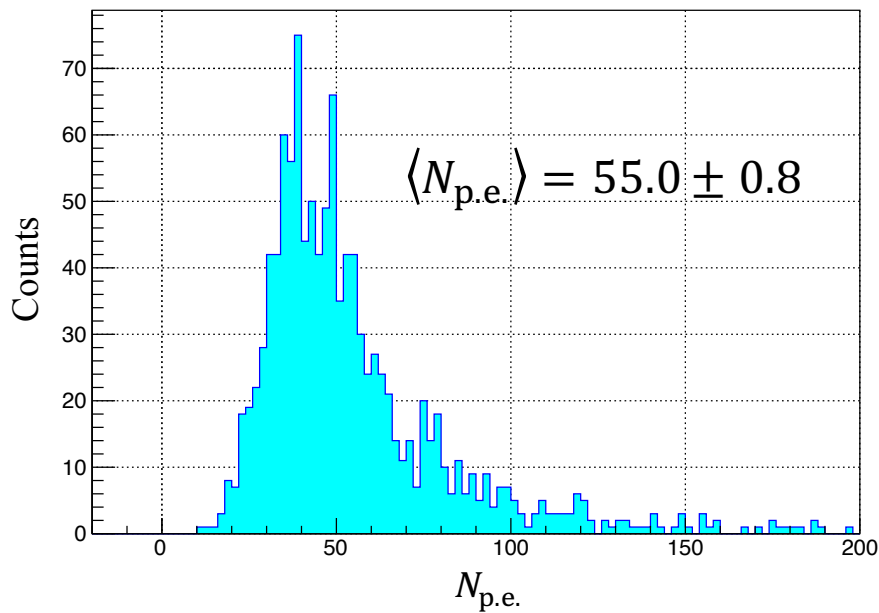
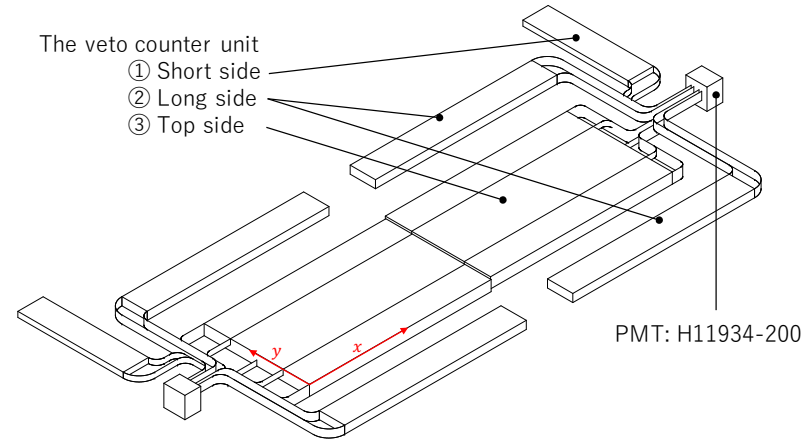


- Photocathode
  - □23 mm
  - Ultra Bialkali
- Metal Channel Dynode



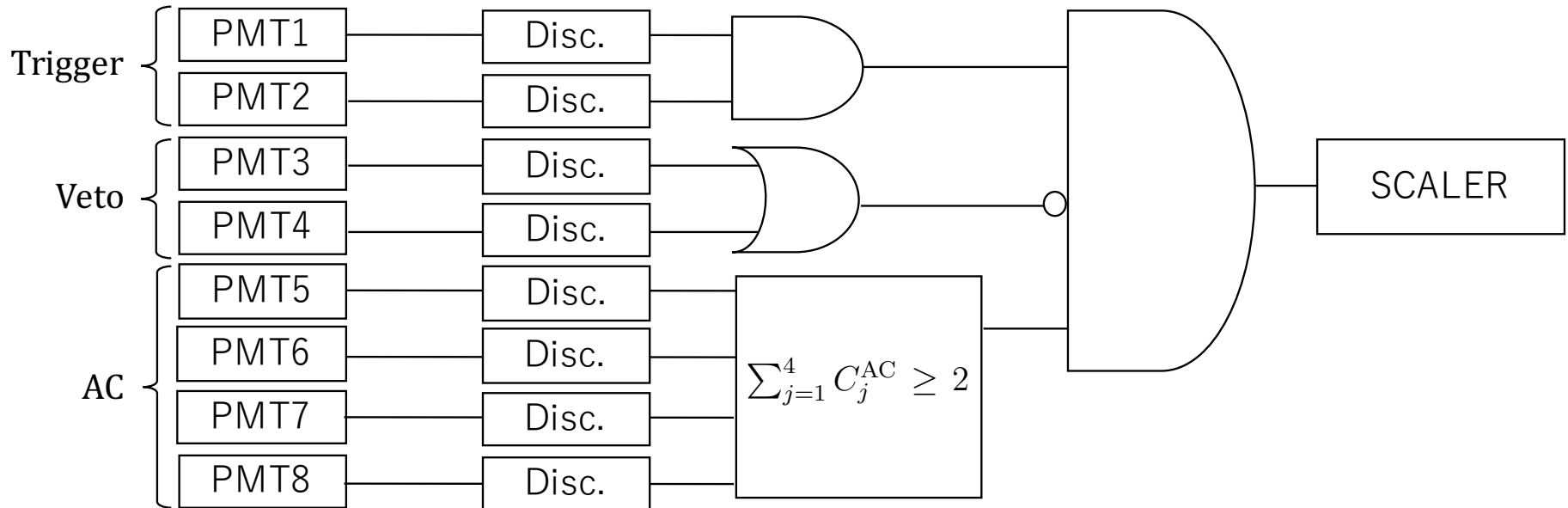
# 4. Design of a prototype detector

## 4.3. Veto counter



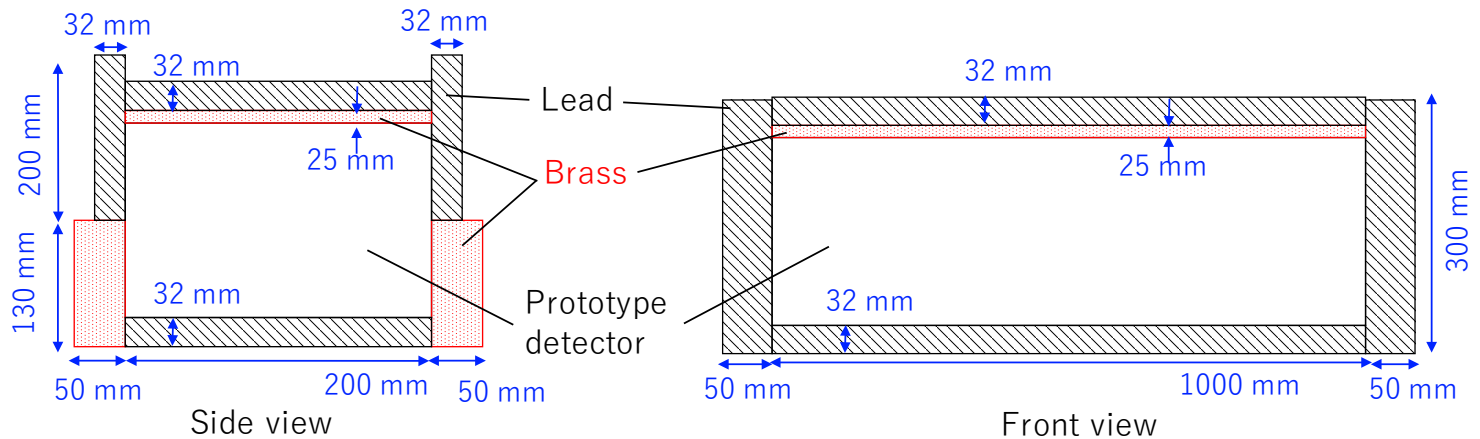
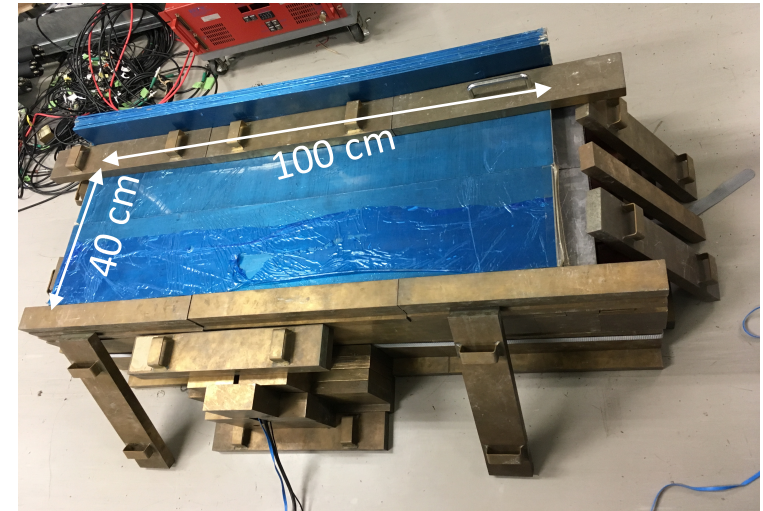
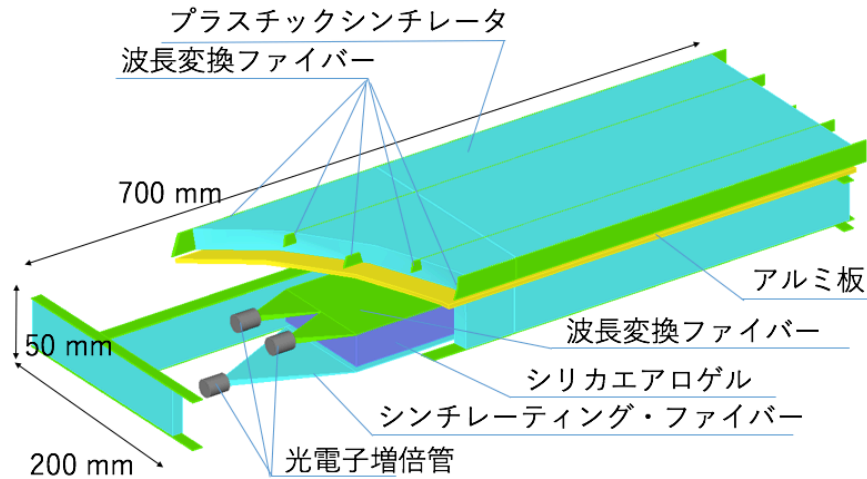
# 4. Design of a prototype detector

## 4.4. Electronics



# 4. Design of a prototype detector

## 4.5. Shielding by lead and brass blocks





## 5. Performance of the prototype detector

## 5. Performance of the prototype detector

### 5.1. Radioactivity of sources

$^{90}\text{Sr}$  source ...  $23.6 \pm 0.3$  kBq

$^{137}\text{Cs}$  source ...  $26.0 \pm 0.5$  kBq

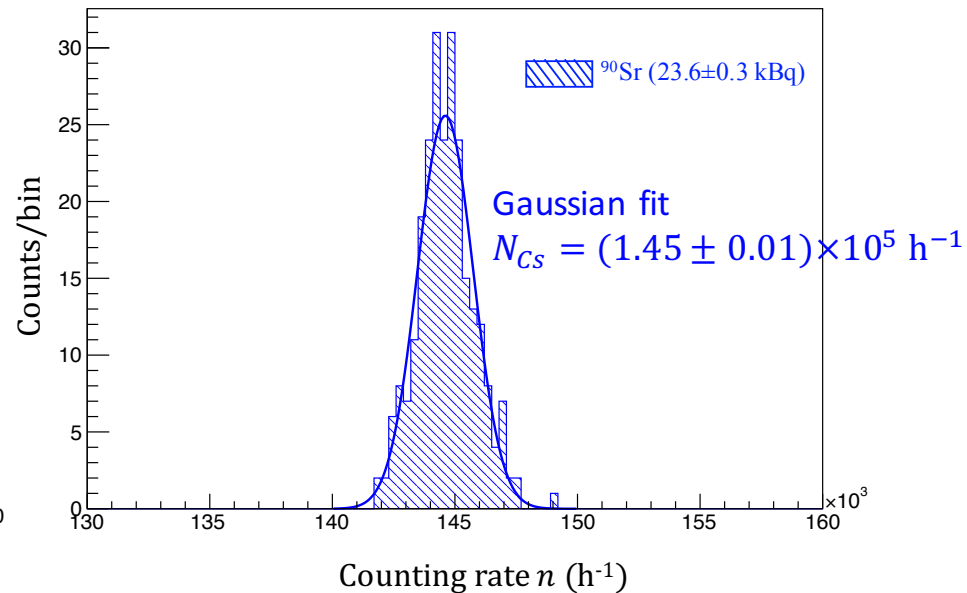
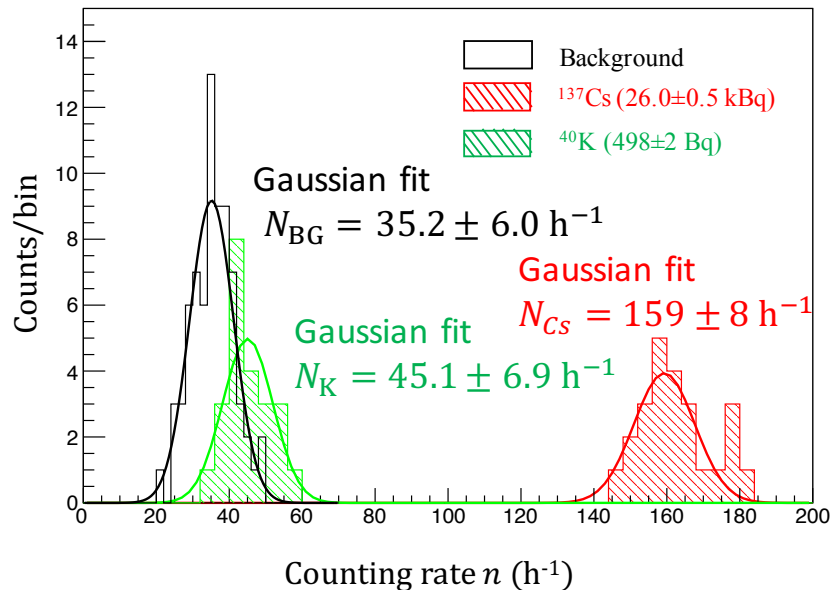
delivered by Japan Radioisotope Association .

$^{40}\text{K}$  source ...  $498 \pm 2$  Bq in potassium chloride (KCl).

The KCl with a mass of  $30.0 \pm 0.1$  g.

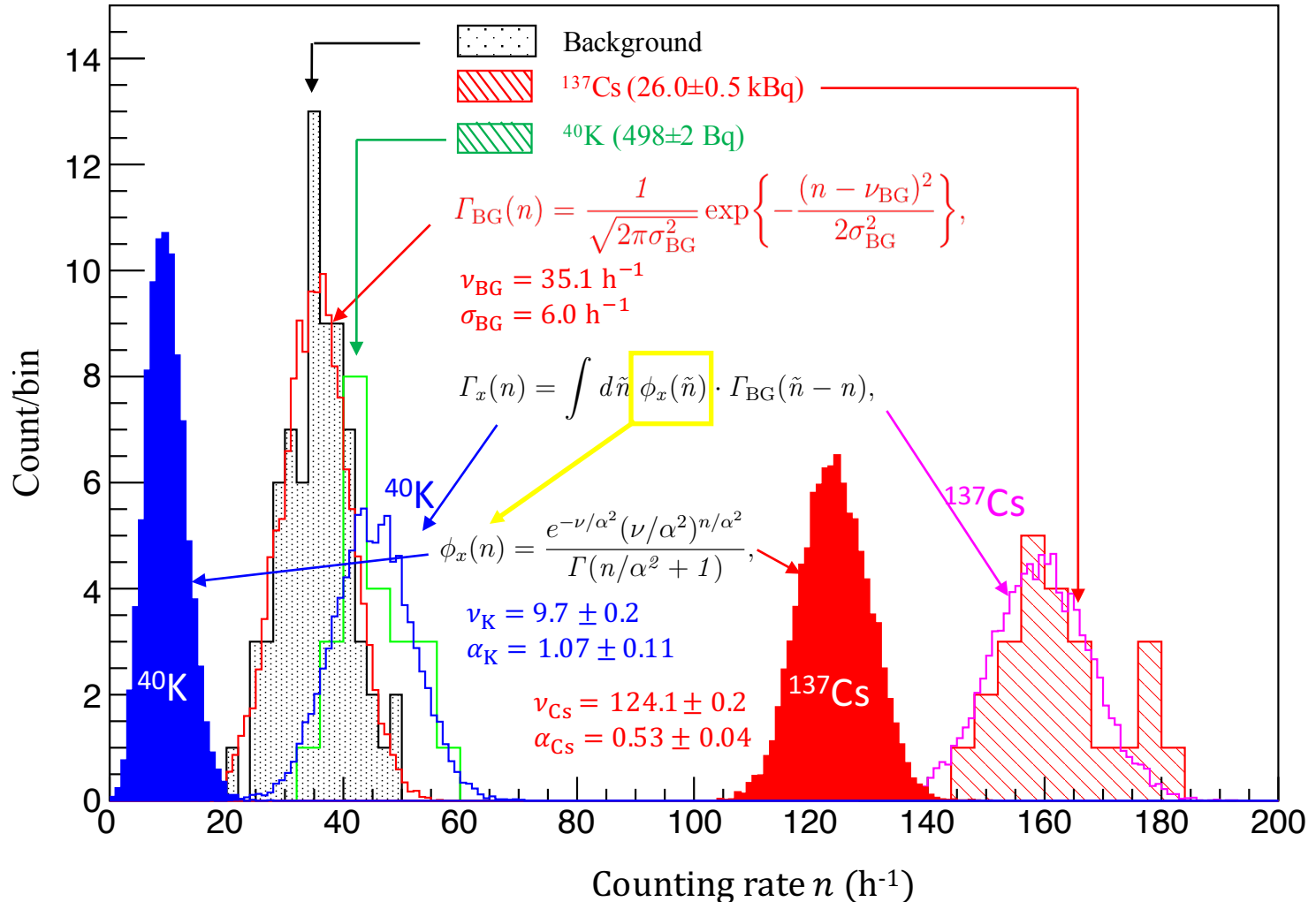
A purity of  $\gtrsim 99.5\%$ .

### 5.2. Counting rate



# 5. Performance of the prototype detector

## 5.3. Signal model



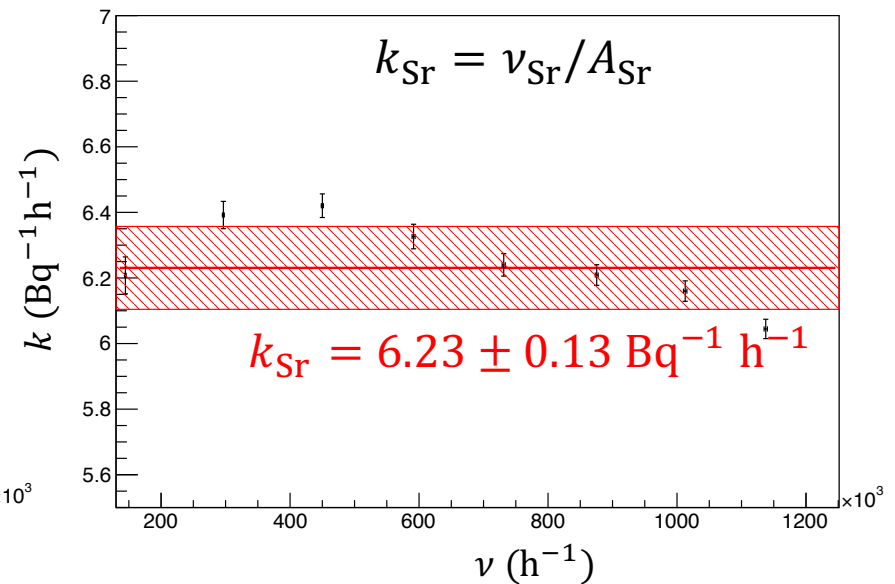
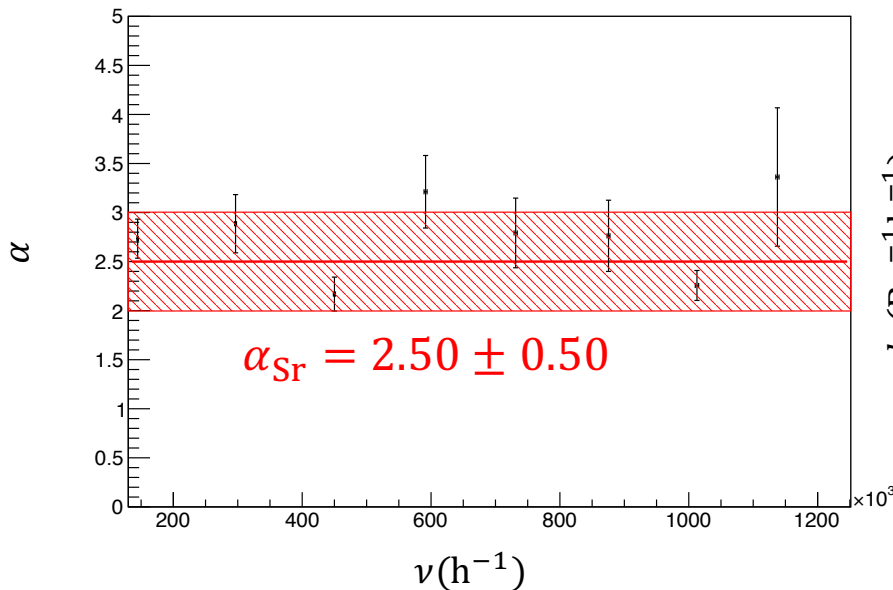
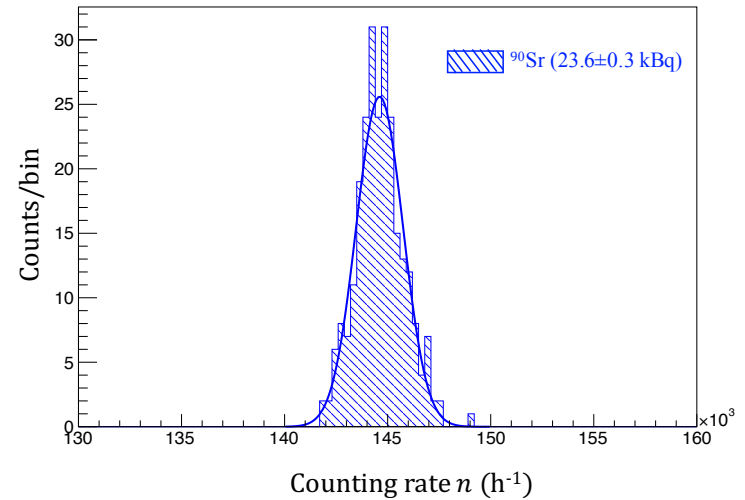
# 5. Performance of the prototype detector

## 5.3. Signal model

$$\langle \Gamma_{BG}(n) \rangle \ll \langle \phi_{Sr}(n) \rangle \Rightarrow \Gamma_{Sr}(n) \approx \phi_{Sr}(n)$$

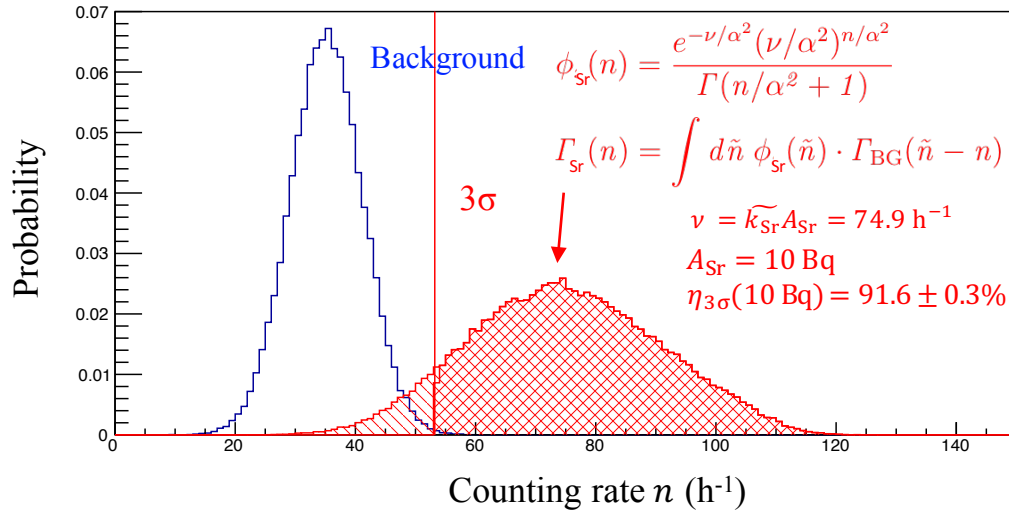
$$\phi_x(n) = \frac{e^{-\nu/\alpha^2} (\nu/\alpha^2)^{n/\alpha^2}}{\Gamma(n/\alpha^2 + 1)}, \quad (x = Sr)$$

Source	$\alpha$	$k$ (Bq <sup>-1</sup> h <sup>-1</sup> )
<sup>90</sup> Sr	2.50 ± 0.50	6.23 ± 0.13
<sup>137</sup> Cs	0.532 ± 0.044	(4.77 ± 0.09) × 10 <sup>-3</sup>
<sup>40</sup> K	1.067 ± 0.106	(1.95 ± 0.04) × 10 <sup>-2</sup>

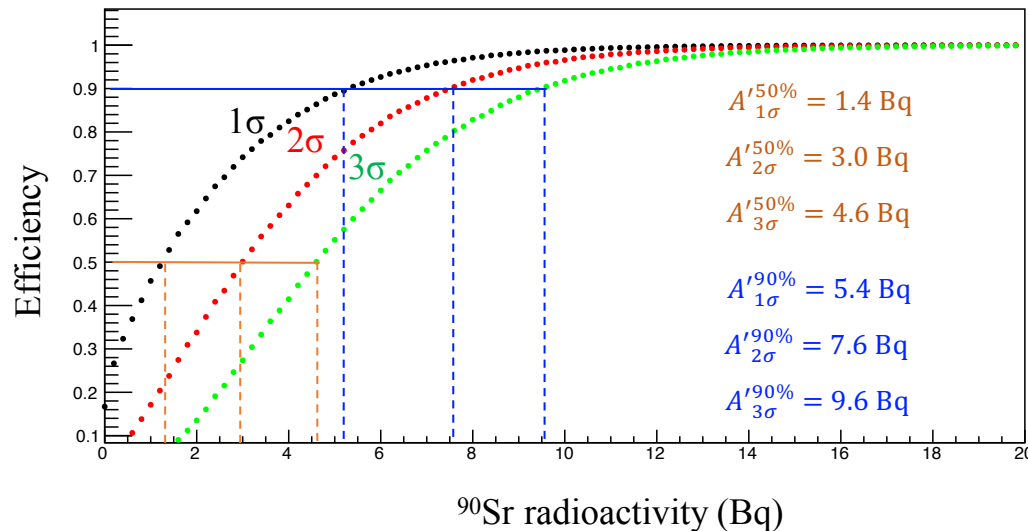


# 5. Performance of the prototype detector

## 5.5. Detection efficiency and limit



- Mean counting rate is  $74.9 \text{ h}^{-1}$  using 10-Bq  $^{90}\text{Sr}$  in the signal model.
- The source position dependence for the coefficient  $k$  was corrected.
- In a case of  $3\sigma$  threshold setting, this detection eff. is estimated to be  $91.6 \pm 0.3\%$  for 10-Bq  $^{90}\text{Sr}$ .



- These curves show relations between  $^{90}\text{Sr}$  radioactivity and the efficiency for 1, 2,  $3\sigma$  threshold condition.
- Typical detection limit is determined to be  $A_{3\sigma}^{50\%}$  satisfying  $\langle \Gamma_{Sr}(n) \rangle > \langle \Gamma_{BG}(n) \rangle + 3\sigma$ .
- $A_{3\sigma}^{50\%} = 4.6 \text{ Bq}$  at 1-hour measuring.

## 5. Performance of the prototype detector

### 5.6. Concentration

Detection limit of surface concentration is  $A_{3\sigma}^{50\%}/S = 0.0153 \text{ Bq/cm}^2$ , where  $S = 300 \text{ cm}^2$ .

Here, it is assumed that

- Density of sample is  $1 \text{ g/cm}^3$
- Sample was dried.
- Compression factor is  $\varepsilon = 0.3$
- Sample thickness is  $1 \text{ mm}$
- Sample weight is  $m = 30 \text{ g}$   
(corresponding to the original  
of  $m/\varepsilon = 100 \text{ g}$ ).

$$A_{3\sigma}^{50\%} m \varepsilon^{-1} = 46 \text{ Bq/kg}$$

at 1-hour measurement.

The food contamination permissible limit of  $100 \text{ Bq/kg}$  defined by Ministry of Health, Labour and Welfare, Japan, in 2012.

$A \propto S^{-1}$ ; it expected to be  $8.4 \text{ Bq/kg}$  @ $S=1 \text{ m}^2$

Furthermore, in the case of seawater, the lower limit of dried seawater in 1-hour measurement is estimated to be  $A_{3\sigma}^{50\%} m \varepsilon^{-1} = 1.5 \text{ Bq/L}$ , where  $\varepsilon = 0.01$ .

## 5. Performance of the prototype detector

### 5.6. Results

- Signal models were developed based on experimental test using the sources.
- The efficiency curves were estimated as the detector performance.
- The detection limit was estimated to be 4.6 Bq.
- The detection limit of surface concentration was estimated to be 0.0153 Bq/cm<sup>2</sup>.
- The detection limit of weight concentration was estimated to be 46 Bq/kg (seafood) and 1.5 Bq/kg (seawater) at 1-hour measurement in the prototype detector.

## 6. Summary

- It is important to measure  $^{90}\text{Sr}$  concentration in food because intake of  $^{90}\text{Sr}$  is dangerous than  $^{137}\text{Cs}$ , and the method of measuring  $^{90}\text{Sr}$  rapidly is focused.
- Wavelength-shifting fiber system was adopted because it is not possible to inspect 10-Bq/kg  $^{90}\text{Sr}$  by a large PMT reading Cherenkov photons directly.
- The light collection efficiency was estimated to be 1.0-1.4% for Cherenkov photons.
- The Cherenkov photons by  $^{90}\text{Y}$   $\beta$  rays was observed using the fibers.
- $^{214}\text{Bi}$  as the radon progenies in the air was not observed in the limit of 100 Bq/m<sup>3</sup>. The radon progenies on the sample sheets was not observed 18 Bq/m<sup>2</sup>. It was found that the detector design should be performed the care for these  $^{214}\text{Bi}$ .
- I produced a prototype detector with an effective area of 30×10 cm<sup>2</sup>.
- The detection limit of weight concentration at 1-hour measurement was estimated to be 46 Bq/kg (seafood) and 1.5 Bq/kg (seawater). By extending to effective area of 1 m<sup>2</sup>, it is expected to be 8.4 Bq/kg (seafood).



# Acknowledgement

I thank to **Prof. Hideyuki Kawai** of Chiba Univ. for providing not only this study but also various precious experiences for a long term of 5 years.

I thank to **Prof. Sigeru Yoshida**, and **Asst. Prof. Keiichi Mase** of Chiba Univ. for providing a chance of this study.

I thank to **Dr. Makoto Tabata** of Chiba Univ. for providing silica aerogel tiles, teaching how to research, and suggesting in this study.

I thank to **Prof. Jun Imazato** and **Dr. Yoichi Igarashi** of High Energy Accelerator Organization (KEK), Japan, **Prof. M. D. Hasinoff** of Univ. of British Columbia, Canada, **Asst. Prof. Suguru Shimizu** and **Dr. Keito Horie** of Osaka Univ., **Asst. Prof. Takatugu Ishikawa** of Tohoku Univ. for grate advices and suggestions.

I thank to **Mr. Satoshi Kodama**, **Mr. Munetaka Nitta**, **Mr. Atsushi Kobayashi**, **Mr. Takahiro Mizuno**, **Mr. Hiroyuki Kobayashi**, **Mr. Taichi Nakamura**, **Mr. Yusaku Emoto**, **Mr. Shota Kimura**, **Mr. Kenta Fujihara**, and **Mr. Kentaro Kurusu** of our good laboratory members in Chiba Univ., for their cooperation.

Finally, I thank to my friends and my family for their special supports.